NATIONAL ADVISORY COMMITTEE
FOR AERONAUTICS

TECHNICAL NOTE

No. 1285

JUN 16 1947.

THEORETICAL MOTIONS OF HYDROFOIL SYSTEMS

By Frederick H. Imlay

Langley Memorial Aeronautical Laboratory
Langley Field, Va.

Washington

June 1947

NATIONAL ADVISORY COMMITTEE FOR AERONAUTICS

TECHNICAL NOTE NO. 1285

THEORETICAL MOTIONS OF HYDROFOIL SYSTEMS

By Frederick H. Imlay

SUMMARY

Results are presented of an investigation that has been under-
taken to develop theoretical methods of treating the motions of
hydrofoil systems and to determine some of the important parameters.
Variations of parameters include three distributions of area
between the hydrofoils, two rates of change of downwash angle with
angle of attack, three depths of immersion, two dihedral angles,
two rates of change of lift with immersion, three longitudinal
hydrofoil spacings, two radii of gyration in pitching, and various
horizontal and vertical locations of the center of gravity. Graphs
are presented to show locations of the center of gravity for stable
motion, values of the stability roots, and motions following the
sudden application of a vertical force or a pitching moment to the
hydrofoil system for numerous sets of values of the parameters.

The lateral stability of tandem-hydrofoil systems is briefly
discussed, and values of the lateral stability roots are presented
for two longitudinal hydrofoil spacings and two vertical locations
of the center of gravity.

The analysis indicates that if only the longitudinal motions
of a hydrofoil system are of interest the present theory should
provide satisfactory predictions. An adequate theory for the
lateral motions, however, must treat the longitudinal and lateral
motions in combination. The conclusions based on the investigation
are that a large longitudinal spacing between the hydrofoils, a
large rate of change of lift with depth of immersion, and a horizontal
location of the center of gravity near the center of the region of
stable locations are important contributions in the attainment of
desirable characteristics for the longitudinal motion. An appendix
gives an outline of the methods of theoretical treatment used and
presents methods used in computing the required stability derivatives.

INTRODUCTION

The use of hydrofoils as an alternative to planing bottoms or hulls for the support of craft operating on the surface of water has been of interest for some time. (See reference 1.) Guidoni advocated the use of hydrofoils as a means of improving the take-off and rough-water performance of seaplanes as early as 1911. (See reference 2.) Some of the advantages claimed for hydrofoils over planing bottoms are a better ratio of lift to drag on the water and less sensitivity to irregularities of the water surface. In addition, if hydrofoils are used, the hull lines can be designed to favor good aerodynamic rather than good hydrodynamic characteristics, and by retracting the hydrofoils the aerodynamic performance can be even further improved. In spite of the evident advantages of these devices and the attention that they have received, no published work is known to exist on the stability of motion for systems employing hydrofoils.

The present paper deals theoretically with the behavior of a system supported solely by hydrofoils and is a first approach to the problem of developing methods of theoretical treatment for the more general case where the interaction of hydrofoils, hull, and aerodynamic surfaces have to be taken into account. The treatment is based on the theory of small oscillations and involves assumptions customarily made in applying the theory. (See reference 3.)

Definitions of all symbols used are listed at the beginning of the appendix.

LONGITUDINAL MOTIONS

The longitudinal motions of a number of hypothetical hydrofoil systems were investigated by means of calculations based on the theoretical treatment presented in the appendix. All the computations were for systems composed of two similar hydrofoils of rectangular plan form and rectangular tips. The hydrofoils were arranged in tandem and had an aspect ratio of 6 and a total hydrofoil area of 0.188 square foot. (See fig. 1.) The systems were assumed to have a mass of 0.256 slug and to operate at a velocity of 20 feet per second in water having a density of 1.97 slugs per cubic foot. The mass of the system was assumed to include all items such as structure and additional mass effect. For systems with dihedral the hydrofoil area, aspect ratio, and span were based on the part of the hydrofoil immersed during the initial undisturbed motion, although unwetted

parts of the hydrofoils were assumed to project above the water far
enough to ensure that the tips were never immersed during disturbed
motions. (See fig. 2.) Most of these dimensional characteristics
of the hydrofoil systems were chosen to facilitate comparison of the
theoretical motions with the results of contemplated experimental tests.
Changes in the other parameters were made to determine their effects
on the stable regions, the stability roots, and the motions resulting
from disturbances.

Effect of Parameters on Stable Regions

The stable region, as used in the present paper, indicates
permissible locations of the center of gravity relative to the
hydrofoils if the longitudinal motions are to be stable. The stable
region alone, however, gives no quantitative indication of the
degree of stability. The stable region is bounded by lines that
are the loci of center-of-gravity locations for which neutrally
stable longitudinal motions occur. The positions of the boundary
lines, and hence the size of the region, vary with changes in the
parameters of the hydrofoil system and thus suggest variations of
the parameters that may be of practical interest for more detailed
study.

The type of unstable motion occurring just outside the boundaries
has been noted for each of the stable regions in figures 3 to 9;
thus, for each stable region, center-of-gravity locations beyond the
rear boundary lead to an unstable divergence, and in most cases
unstable oscillations occur for locations beyond the front boundary.
The rear boundary is always located farther to the rear of the front
hydrofoil than would be the case for a similar pair of airfoils
because of the additional damping introduced as a result of the
sensitivity of the hydrofoils to depth of immersion.

In addition to the selection of a center-of-gravity location
that lies within the stable region in order to meet the requirements
for stability, certain supplementary practical factors must be
considered. For example, negative lift on either hydrofoil should
be avoided; otherwise momentary uncovering of the hydrofoil (as by
a wave trough) will be followed by nosing-over if the rear hydrofoil
is operating at negative lift, or nosing-up if the front hydrofoil
is operating at negative lift. Furthermore, the longitudinal
location of the center of gravity is also restricted by the maximum
positive lift obtainable, and may be influenced by the desirability
of operating the hydrofoils near their maximum lift-to-drag ratios.
The net effect of such restrictions is to reduce the usable part of
some of the computed stable regions shown in figures 3 to 9.

In the present study, where the effects of power are neglected, the vertical center-of-gravity location selected appears to be of secondary importance, low locations being somewhat advantageous. The effects of power, however, will undoubtedly have an important bearing on the choice of the vertical center-of-gravity location.

Distribution of area.- The effect of the distribution of area between the two hydrofoils on the extent of the stable region is shown in figure 3. The plan-form arrangements assumed for the three distributions treated are shown in figure 1. In arrangement 1 the hydrofoils were identical; in the other two arrangements the ratio of the distribution of area was 1:4 and the arrangements differed only in the location of the larger hydrofoil. All the arrangements had the same total hydrofoil area of 0.188 square foot. The horizontal distance between the assumed hydrodynamic centers of the hydrofoils for all arrangements was $10.0c_1$, where c_1 is the chord for the arrangement with two equal hydrofoils, and the assumed hydrodynamic center was located at the quarter-chord point of the center section. All the hydrofoils were assumed to be immersed $1.0c_1$ at the hydrodynamic center during the initial undisturbed motion.

Figure 3 shows that the configuration with the small surface ahead (arrangement 3) gave the largest useful stable region. The rearward extent of the stable region for the arrangement with two hydrofoils of equal area (arrangement 1) was considered adequate, however, and because this arrangement permitted certain simplifications in the calculations, it was used for the rest of the work. The configuration having the main surface ahead (arrangement 2) would, from theoretical considerations, be the most efficient arrangement for developing lift but has a considerably more limited range of stable center-of-gravity location than do the other arrangements.

Rate of change of downwash.- In a tandem-hydrofoil system the downward velocity produced in the fluid by the front hydrofoil reduces the effective angle of attack of the rear hydrofoil by the amount of the downwash angle ϵ. The downwash angle is a function of the lift on the front hydrofoil and hence varies with angle of attack. The rate of change of downwash angle with angle of attack, which is the factor of interest from the standpoint of stability, will be represented by the symbol ϵ_α. The value of ϵ_α will probably be intermediate between zero and the theoretical ultimate maximum $\epsilon_\alpha = \dfrac{2}{\pi A_1} \dfrac{\partial (C_L)_1}{\partial \alpha_1}$ but to determine the value accurately would require an investigation of downwash near a free surface. Corresponding limiting values of ϵ, which are given instead of ϵ_α in the figures for the sake of brevity, are zero and twice the induced angle of attack α_i. In order

to show the influence of the rate of change of downwash on the
nature of the stable region, computations were made for these two
extremes, and the results for a system having two equal hydrofoils
are shown in figure 4. An increase in the variation of downwash
with α shifts both boundaries forward without appreciably altering
the size of the stable region.

The effect of downwash for the other hydrofoil arrangements was
found to be similar to that indicated by figure 4 for the arrangement
with two equal hydrofoils. Because there was no pronounced change
in the size of the stable region with change in downwash, the
condition of zero rate of change of downwash with α was assumed in
most of the remaining calculations.

The true boundaries of the stable region for the system treated
in figure 4 lie somewhere within the bands defined by the boundaries
for $\epsilon = 0$ and $\epsilon = 2\alpha_1$, but accurate definition of the boundaries
requires that ϵ be known. Conservative estimates will be obtained,
when the value of ϵ is not known, if the assumptions are made that
$\epsilon = 2\alpha_1$ for computing the location of the rear boundary and that
$\epsilon = 0$ for the front boundary.

Depth of immersion.- The lift and drag obtained from a hydrofoil
depend upon the depth of immersion z_0 of the hydrofoil in the water.
Because appreciable change in the depth of immersion may occur under
normal operating conditions, computations of the stable region were
made for immersion depths of $0.5c_1$, $1.0c_1$, and $1.5c_1$. (See fig. 5.)
Limits of the stable region were not altered to any important extent
by the assumed changes in the depth at which the hydrofoils operate.

Dihedral angle.- The effect on the stable region of increasing
the dihedral angle Γ of the hydrofoils from $0°$ to $30°$ is shown in
figure 6. Both the front and the rear boundaries of the stable
region were affected by the dihedral in such a way that the increase
in dihedral increased the size of the stable region.

Increasing the dihedral angle from $0°$ to $30°$ resulted in an
associated increase in vertical damping. It appeared reasonable
that the improved stability obtained by changing the dihedral might
have resulted from this increased vertical damping; consequently
the effect of arbitrarily increasing the vertical damping for the
hydrofoils with a dihedral angle of $0°$ was studied and the results
are discussed in the next section.

Rate of change of lift with immersion.- If the depth of immersion
of a hydrofoil is changing, the lift is also changing, and the rate
of change can be expressed by the vertical-damping derivative $\partial C_L/\partial z'$.
It is believed that the increased stability which accompanied the

increase in dihedral angle from $0°$ to $30°$ (discussed in the preceding
section) may have been brought about by the resulting increase in
the value of $\partial C_L/\partial z'$. Inasmuch as a further increase in dihedral
angle would decrease the value of the derivative, an explanation of
the increase in $\partial C_L/\partial z'$ when the dihedral was changed from $0°$ to $30°$
may be of interest.

In order to avoid the mathematical difficulties of treating
discontinuous derivatives the assumption was made in the present
study, for the case of hydrofoils with dihedral, that a normally
inactive part of the hydrofoil extended sufficiently far above the
water surface to keep the hydrofoil from being completely immersed
at any time during disturbed motion. (See fig. 2.) As a result of
this assumption, hydrofoils with dihedral have a larger variation of
lift with change in depth of immersion than do hydrofoils with
$0°$ dihedral because of the increased area brought into action when
the hydrofoil sinks deeper into the water. This variation in active
area becomes greater as the dihedral angle becomes smaller.

The effect on the stable region of increasing the value of
$\partial C_L/\partial z'$ for each hydrofoil to twice the value that the hydrofoils
had with $30°$ dihedral, but having other characteristics the same as
for $0°$ dihedral, may be seen by comparing figures 6 and 7. Doubling
the value of $\partial C_L/\partial z'$ shifts the rear boundary of the stable region
back considerably and produces pronounced changes in the front
boundary. The former boundary for unstable oscillations now becomes
an unstable "hump" in the region with a new front boundary ahead of
the hump. The new forward boundary represents conditions for an
unstable divergence, but the boundary is too far ahead of the front
hydrofoil to be of any practical interest.

Longitudinal hydrofoil spacing.- The effect on the stable
region of increasing the longitudinal spacing of the hydrofoils from
$10c_1$ to $20c_1$ is shown in figure 8. The larger spacing results in a
very large increase in the stable region and in the replacement of
the front boundary that indicated unstable oscillations by a new
front divergent boundary. The new front boundary is well ahead of
the front hydrofoil, which is the practical limit of forward center-
of-gravity location.

The absence of a boundary for oscillatory instability for the
system with a spacing of $20c_1$ suggests that the large amount of
damping in pitching for this spacing, relative to the pitching radius
of gyration K_Y, might result in overdamping and thus prevent the
system from having any oscillatory motion. Calculations with K_Y
reduced to give a similar relation between inertia and damping for
the small spacing of $10c_1$, made to check the hypothesis, showed that
oscillations were still obtained; thus, it appears that the absence

of unstable oscillations for the larger spacing does not signify inability of the system to have transient oscillations.

The pronounced increase in the size of the stable region when the longitudinal spacing of the hydrofoils is increased indicates that a large spacing is desirable in order to minimize the effects of unavoidable changes in center-of-gravity location encountered in practice. In a previous section entitled "Distribution of Area" a spacing of $10c_1$ was used in the calculations made to study the effects of distribution of area. If a larger spacing had been used, it would possibly have resulted in a sufficient gain in the size of the stable region for the arrangement with the large hydrofoil forward to make this configuration of practical value.

Radius of gyration in pitching.- The marked increase in permissible horizontal center-of-gravity movement when K_Y is reduced is indicated in figure 9, where the stable range of horizontal center-of-gravity location is shown for zero vertical elevation of the center of gravity with K_Y reduced to one-fourth the value used previously. The pronounced effects of reducing K_Y indicate that increased values of K_Y, which are more likely to be used, should receive attention because of possible adverse effects on the characteristics of the longitudinal motions.

Effect of Parameters on Stability Roots

When the equations of motion are solved, the motion is obtained as the sum of a series of components called modes. Stability roots, which indicate the degree of stability of the various modes, can also be obtained from the equations of motion without effecting a complete solution of the equations. A more detailed discussion of the significance of the stability roots is contained in the appendix of reference 4. Information obtained from the stability roots is most useful when the relative magnitude or importance of the various modes is known, because the roots then provide a clue to the nature of the complete motion.

In the present analysis, four stability roots λ are obtained from the longitudinal equations of motion and are distinguished by the subscripts 1 to 4. The nature of the roots changes with variations in the parameters of the hydrofoil system. A typical variation in the real parts of the roots is shown in figure 10. In general, when the magnitudes of any two real roots become equal, the two real roots are replaced by a conjugate pair of complex roots, each having the same magnitude for the real part. Thus, such pairs of complex roots in figure 10 are indicated by a double line and an appropriate modification of the subscript. The magnitude of the real

part for such complex pairs of roots should be read off the plots at the center of the double line.

For every real root obtained from the equations of motion the complete solution will contain an aperiodic mode, or component, of the motion. Likewise, for every pair of complex roots the motion will contain an oscillatory component. When the magnitude of the real part of any of the roots passes through zero, the motion becomes unstable.

Horizontal center-of-gravity location.- The effect of changing the horizontal location of the center of gravity on the real parts of the stability roots is shown in figure 10 for a system of two equal hydrofoils with 30° dihedral. For center-of-gravity locations ahead of the hydrodynamic center of the front hydrofoil, two real roots λ_1 and λ_2 and a pair of complex roots $\lambda_{3,4}$ exist. When the center of gravity is $2.16c_1$ ahead of the front hydrofoil the $\lambda_{3,4}$ roots are unstable, which indicates that the center of gravity has reached the forward boundary of the stable region. As the center of gravity is moved rearward, the stability slowly improves for the oscillatory component of the motion represented by the $\lambda_{3,4}$ roots. Meanwhile the magnitudes of the λ_1 and λ_2 roots approach each other and become equal when the center of gravity is about $1.5c_1$ behind the front hydrofoil. With farther rearward movement of the center of gravity the roots are coupled as two oscillations represented by $\lambda_{1,2}$ and $\lambda_{3,4}$. When the center of gravity is moved back to the vicinity of $4.5c_1$ behind the front hydrofoil rather rapid changes in coupling occur, which finally result in a real root λ_1 with a large amount of damping, a complex pair $\lambda_{2,3}$ with moderate damping, and a real root λ_4 with slight damping. When the center of gravity is moved back to a point $5.49c_1$ behind the front hydrofoil, the magnitude of the λ_4 root becomes zero and the rear boundary of the stable region has been reached.

The behavior of the roots as the horizontal location of the center of gravity is changed indicates that the type of motion caused by disturbances will be considerably influenced by the longitudinal location of the center of gravity.

Rate of change of downwash.- The effect on the stability roots of assuming the downwash angle ϵ to be $2\alpha_1$ instead of zero can be seen from a comparison of figures 10 and 11. No pronounced change in the roots occurred with variation in ϵ_α, except for a shift of the pattern of root couplings with respect to the horizontal center-of-gravity location; this result is consistent with indications obtained earlier from a study of the influence of ϵ_α on the stable region. Hence, for the rest of the work the value of ϵ_α was assumed to be zero.

Dihedral.- The influence on the stability roots of changing the dihedral angle from $30°$ to $0°$ is evident when figure 10 is compared with figure 12. The difference in the rate at which the $\lambda_{2,3}$ oscillation develops with rearward center-of-gravity movement for the two dihedral angles accounts for the different appearance of the right side of the diagram in the two figures. The most important feature disclosed by the comparison is the improvement, brought about by the use of dihedral, in damping of the component of motion involving the root λ_4 or the complex pair $\lambda_{3,4}$.

Vertical center-of-gravity location.- Figures 13 and 14 together with figure 10 show the effect on the stability roots of varying the vertical center-of-gravity location from a point on a level with the hydrofoils to a point $10c_1$ above the hydrofoils. As had been indicated by the diagrams of the stable regions, no pronounced changes occur in the nature of the roots when the vertical center-of-gravity location is shifted.

Rate of change of lift with immersion.- The effect on the stability roots of making the value of $\partial C_L/\partial z'$ twice that for $30°$ dihedral is evident if figure 15 is contrasted to figure 10. Doubling the vertical-damping derivative caused marked improvement in the $\lambda_{3,4}$ oscillation, which suggests that the similar improvement in damping obtained by increasing the dihedral angle from $0°$ to $30°$ was a result of the associated increase in the value of $\partial C_L/\partial z'$.

Effect of Parameters on Indicial Responses

An indicial response is the motion resulting from a unit force or moment suddenly applied to the hydrofoil system at zero time and held constant thereafter. The indicial responses are of interest because they are of the same general character as the motions produced by types of disturbance that are likely to be encountered in practice.

The longitudinal equations of motion (equations (9)) involve three variables; hence three indicial responses are necessary to define the motion caused by any specific unit disturbance. The three indicial responses may be conveniently represented by the symbols α_z, z'_z, and θ_z for the change in angle of attack, vertical position, and angle of pitch, respectively, when the motion is caused by the sudden application of a unit C_z-force to the hydrofoil system. Similarly α_m, z'_m, and θ_m are the response factors for a sudden unit C_m disturbance.

The indicial responses are functions of nondimensional time s_c, typical variations of which are shown in figure 16. The magnitude of disturbances actually encountered, when expressed in coefficient form, will usually be considerably less than unity; consequently, the actual motions experienced will be of proportionately smaller magnitude than the indicial responses presented but will have the same type of variation with time. Values of the indicial responses after the disturbance has been absorbed by the system and new steady-state equilibrium conditions have been reached are represented by short horizontal lines at the right side of the plots. Such steady-state values are not only new equilibrium conditions for sudden disturbances but also represent new trim conditions after gradual changes in the load condition, such as would result from the use of fuel.

Horizontal center-of-gravity location.- Indicial responses for a unit C_Z-disturbance applied to a system of two equal hydrofoils with zero dihedral are plotted against nondimensional time in figure 16 for several horizontal locations of the center of gravity. Values of x_1 used in figure 16 were selected to give center-of-gravity locations covering all the types of root coupling shown in figure 12. If the center-of-gravity locations used in figure 16 are noted on the diagram of the corresponding stable region (see fig. 3), the following points are evident:

(1) A center-of-gravity location near the front boundary of the stable region is conducive to motions characterized by pronounced oscillations.

(2) A more rearward location of the center of gravity reduces the prominence of the oscillations but increases the ultimate deviation from the attitude that existed before the disturbance.

(3) For center-of-gravity locations near the rear boundary, no discernible oscillation is noted, but very large departures from the initial condition occur.

Comparison of the maximum deviations for the three center-of-gravity locations of figure 16 shows that, during the interval of time covered by the curves, the smallest amplitude of motion of the hydrofoil system occurs for the case with the center of gravity back 35 percent of the distance l between the two hydrofoils. The deviation caused by a given disturbance rapidly becomes greater as the center of gravity is moved back of the optimum location, with the result that for such rearward locations a very slight disturbance would bring the hydrofoils to the surface or cause them to sink very deep into the water. Location of the center of gravity any appreciable distance ahead of the optimum location appears undesirable because of the pronounced oscillatory motions involved. Such motions would be both uncomfortable and difficult to control.

Indicial responses for a unit C_m-disturbance, for the same conditions as for figure 16, are plotted in figure 17. The discussion of the effect of change in horizontal center-of-gravity location on the indicial responses for a unit C_z-disturbance also applies for a unit C_m-disturbance, with the exception that the amplitudes of the motions are least for the most forward center-of-gravity location considered, instead of for the middle location. The oscillations are much more persistent, however, for the forward location than for the middle location.

Because of the large response factors involved for either type of disturbance, even when the best center-of-gravity location is selected, motions for hydrofoils with no dihedral will involve large amplitudes whenever a slight disturbance is encountered; hence, it appears evident that such a type of hydrofoil will not give satisfactory performance. This conclusion applies only to the arrangement investigated, where the hydrofoils always remain completely submerged, and it should not be extended to cover ladder arrangements, for which a change in effective area with immersion depth produces effects similar to those for partly immersed hydrofoils with dihedral.

Dihedral angle.- The effect on the indicial responses of increasing the dihedral angle from 0° to 30° may be obtained by a comparison of figures 18 and 16 for a unit C_z-disturbance, and of figures 19 and 17 for a unit C_m-disturbance. The figures indicate that the effect on the nature of the motions of changing the horizontal center-of-gravity location is much the same as that indicated in the preceding parts of the present paper. Thus, the most desirable center-of-gravity location appears to be about $3.50c_1$ back of the front hydrofoil, as in the case for 0° dihedral angle. At any particular horizontal location of the center of gravity the increase in dihedral causes an appreciable reduction in the indicial responses. The reduced sensitivity to disturbances when the dihedral angle was increased from 0° to 30° may have been a result of the corresponding increase in vertical damping. In such a case, as mentioned in the discussion of stable regions, a further increase in dihedral would have an effect opposite to that caused by this initial increase in dihedral.

Rate of change of lift with immersion.- The effect of varying the rate of change of lift with immersion on the indicial responses for a unit C_z-disturbance may be seen from a comparison of figures 16, 18, and 20. Figures 16 and 18 give the indicial responses for hydrofoils with dihedral angles of 0° and 30°, respectively; whereas for figure 20 the rate of change of lift with immersion is assumed to have a value twice that for hydrofoils of 30° dihedral angle but to have other hydrofoil characteristics the same as for 0° dihedral angle. If the case for the center of

gravity at $3.50c_1$ is selected in each of the figures, comparison
shows the direct relation between good riding characteristics and
a large value of $\partial C_L/\partial z'$. It appears, therefore, that a large
value of $\partial C_L/\partial z'$ should be attained by the use of arrangements
such as hydrofoils with dihedral for which the effective area
changes with immersion depth, or by the use of some device that
changes the angle of attack when the height varies. Figure 21
gives data corresponding to the data of figure 20, but with a
unit C_m-disturbance assumed. Results for the several center-of-
gravity locations assumed in figures 20 and 21 indicate the same
influence of horizontal center-of-gravity location on the motions
as has been shown by the computations summarized in figure 17.

Longitudinal hydrofoil spacing.- Indicial responses for either
a unit C_z-disturbance or a unit C_m-disturbance applied to a
system of two equal hydrofoils spaced $20c_1$ are given in figure 22.
The horizontal center-of-gravity location in figure 22 is at $0.35l$,
which is the same percentage of l that was used in figures 18
and 19, and other conditions are also the same as for figures 18
and 19. Figure 23 gives data similar to the data of figure 22
except that the spacing has been increased to $100c_1$. Comparison of
figures 18, 19, 22, and 23 indicates that increasing the hydrofoil
spacing tends to increase the restraint in pitching and thus
reduces the response in all degrees of freedom for pitching-moment
disturbances, and in all but vertical motions for Z-force disturbances.
The effect of increasing the hydrofoil spacing on the motions suggests
that the spacing should be as large as is practical, in order to
reduce the response to a given disturbance. Figure 24 shows the
significance of $10c_1$, $20c_1$, and $100c_1$ spacings if the hydrofoil
systems were attached to a typical flying boat.

LATERAL MOTIONS

Lateral stability for flying boats has not generally been a
serious problem up to the present time; hence the present investiga-
tion of the lateral characteristics of hydrofoils was brief and
made chiefly to check the lateral stability of typical hydrofoil
arrangements assumed in much of the study of longitudinal stability.

In the present investigation all the lateral stability
calculations were made for a hydrofoil system consisting of two
identical hydrofoils of rectangular plan form, each having
rectangular tips, $30°$ dihedral, and an aspect ratio of 6. The
center of gravity was assumed to have a horizontal location $0.35l$
behind the hydrodynamic center of the front hydrofoil. The rate
of change of downwash at the rear hydrofoil was assumed to be zero.

The mass of the hydrofoil system was the same as that assumed for the investigation of longitudinal stability. The study was confined to what was considered the idealized case, where the supporting struts have no influence on the characteristics of the hydrofoil system. The method of treatment for the lateral motions was similar to that used for the longitudinal motions and is described in detail in the appendix.

The effects of changes in the vertical location of the center of gravity and changes in the longitudinal spacing of the hydrofoils on the lateral stability roots are indicated by the data of the following table:

z_1 (chords)	l (chords)	Lateral stability roots			
2.5	10	0	$-0.544 \pm 1.122i$	$-0.472 \pm 0.204i$	
5.0	10	0	$-1.715 \pm 0.523i$	$-0.242 \pm 0.101i$	
5.0	20	0	$-2.274 \pm 1.958i$	-0.221	-0.292

The zero root that is listed for each set of values of z_1 and l in the table results because the system is insensitive to heading; that is, the performance does not depend on the initial direction of travel. The remaining roots listed are either negative or have negative real parts in the case of complex roots, which indicates that all the systems investigated were laterally stable. Instability was expected in the two cases with the higher center-of-gravity location, but apparently the stabilizing effect of the rolling moment that is developed when the system is banked (defined by the value of the derivative $\partial C_l/\partial \phi$) outweighs the effect of the higher center-of-gravity location. Check calculations made with $\partial C_l/\partial \phi$ reduced to nearly zero but with other conditions the same as for the second case in the table showed pronounced lateral instability. From the foregoing results the value of $\partial C_l/\partial \phi$ appears to have an important influence on lateral stability. The value of this derivative is likely to depend on the depth of immersion of the hydrofoils; therefore it may impose a coupling between the longitudinal and the lateral motions and thus prevent reliable predictions of the lateral behavior when the longitudinal motion is ignored. In contrast, none of the longitudinal derivatives appears to be appreciably affected by lateral motions.

The data given in the table indicate that raising the center
of gravity and increasing the longitudinal spacing of the hydrofoils
both increase the total damping in the hydrofoil system, but the
practical value of the increase in damping cannot be determined
except from a study of the response factors involved. Such a study
does not seem feasible until experimental checks are made on the
validity of certain of the assumptions made in developing the theory
for lateral motions.

SUGGESTIONS FOR FUTURE RESEARCH

The present study is based on the assumption of small
displacements. Because of the nonlinearity of many of the derivatives
involved, any appreciable departures from the assumed speed, depth of
immersion, and other factors may cause marked changes in the dynamic
characteristics of the system. Studies of maneuvers, such as take-
offs, of hydrofoil systems may consequently require step-by-step
treatment. The development of methods of studying the combined
motions and determination of the effects of changes in forward speed,
hydrofoil loading, and moments of inertia on the motions also appears
desirable. For seaplanes the interaction of hydrofoils, hull, and
aerodynamic surfaces must be considered. Other factors that should
receive attention are the influence of the hydrofoil supports
(particularly on lateral motion), the effects of power, and the
nature of the downwash near a free surface.

CONCLUDING REMARKS

A theoretical investigation was made of tandem hydrofoil
arrangements, based on the lifting-line theory. The conclusions
which follow apply to only the longitudinal behavior, inasmuch as
the computations made were insufficient to justify definite conclusions
regarding the lateral motions.

1. The longitudinal hydrofoil spacing should be as large as is
feasible.

2. The rate of change in lift with change in depth of immersion
of the hydrofoils should be large. Dihedral appears to be
advantageous, if the hydrofoil is partly immersed, because with
dihedral there is a larger rate of change of lift with change in
immersion. The rate of change of lift with immersion will be
insufficient for hydrofoils with no dihedral unless the area is
composed of several panels in a multiplane arrangement.

3. The rear hydrofoil area should be as large as, or larger than, the front hydrofoil area if large variations in center-of-gravity location are to be accommodated when the longitudinal hydrofoil spacing is small (of the order of 10 chords). With appreciably larger spacings, the arrangement with the main surface forward appears to be sufficiently stable and should be more efficient than the other arrangements.

4. The choice of horizontal center-of-gravity location should be based on considerations of the resultant characteristics of the longitudinal motions and the hydrofoil loading. The location should not be ahead of the hydrodynamic center of the front hydrofoil, in order to avoid undesirable loading. The location should be as far ahead of the rear boundary of the stable region as is feasible without incurring objectionable oscillations. The best compromise from this latter standpoint appears to be a location near the center of the stable region. For two equal hydrofoils in tandem the best location appears to be back about 35 percent of the distance between the hydrofoils.

5. If the effects of power are neglected, the vertical center-of-gravity location appears to be of little importance, low locations being somewhat advantageous.

6. A reduction in the pitching radius of gyration will cause an appreciable increase in the range of horizontal center-of-gravity location that will be stable.

Langley Memorial Aeronautical Laboratory
    National Advisory Committee for Aeronautics
        Langley Field, Va., May 9, 1947

APPENDIX

METHODS OF THEORETICAL TREATMENT

SYMBOLS

h.c.	hydrodynamic center
c.g.	center of gravity of hydrofoil system
X-, Y-, Z-axes	rectilinear reference axes fixed in hydrofoil system, with origin located at center of gravity (The X-axis is alined in the direction of the initially undisturbed motion. The initial position of the Y-axis is directed horizontally to the right. The Z-axis is directed downward.)
X, Y, Z	forces along X-, Y-, and Z-axes, respectively
L, M, N	moments about X-, Y-, and Z-axes, respectively
Z'-axis	axis, directed vertically downward with respect to the earth from origin located at center of gravity of hydrofoil system
Z'	displacement along Z'-axis
ϕ, θ, ψ	angular displacments of reference axes from initial positions, radians (see fig. 25)
α, β	angles, in radians, giving instantaneous orientation of reference axes with respect to path of motion (see fig. 25); thus α is angle of attack and β angle of sideslip at center of gravity
V	linear velocity of center of gravity
Ω	angular velocity of hydrofoil system about center of gravity, radians per second
u, v, w	components of V along X-, Y-, and Z-axes, respectively
p, q, r	components of Ω about X-, Y-, and Z-axes, respectively

W   weight of hydrofoil system

m   mass of hydrofoil system

k_X, k_Y, k_Z radii of gyration of hydrofoil system about respective reference axes

ρ_w density of water

1   subscript used to designate front hydrofoil in a system of two hydrofoils in tandem

2   subscript used to designate rear hydrofoil in a system of two hydrofoils in tandem

S   total projected area of immersed part of hydrofoil system under conditions of steady undisturbed motion

S_n total projected area of nth hydrofoil

c_n chord of nth hydrofoil

b_n span of nth hydrofoil

A_n aspect ratio of nth hydrofoil

Γ_n dihedral angle of nth hydrofoil, in radians unless specified otherwise

Γ dihedral angle when angle is same for all hydrofoils in system

α_n angle of attack at hydrodynamic center of nth hydrofoil, radians

α_i induced angle of attack at hydrodynamic center of front hydrofoil, radians

ϵ downwash angle at hydrodynamic center of rear hydrofoil, radians

ϵ_α rate of change of ϵ with α

ϵ_q rate of change of ϵ with qc_1/V

β_n angle of sideslip at hydrodynamic center of nth hydrofoil, radians

$\left(\dfrac{pb}{V}\right)_n$ nondimensional rolling velocity at hydrodynamic center of nth hydrofoil, based on local rolling velocity in radians per second, b_n, and V

$\left(\dfrac{rb}{V}\right)_n$ nondimensional yawing velocity, with definition similar to that for $\left(\dfrac{pb}{V}\right)_n$

C_L lift on hydrofoil system, measured at center of gravity in direction perpendicular to V and converted to coefficient form by dividing by $\frac{1}{2}\rho_w V^2 S$

C_{L_n} lift on nth hydrofoil, measured at hydrodynamic center of hydrofoil under consideration in a direction parallel to C_L and converted to coefficient form by dividing by $\frac{1}{2}\rho_w V^2 S$

$\left(C_L\right)_n$ lift on nth hydrofoil, measured at hydrodynamic center of hydrofoil under consideration in direction perpendicular to local relative motion and converted to coefficient form by dividing by $\frac{1}{2}\rho_w V^2 S_n$

$\left(C_D\right)_n$ drag on nth hydrofoil, measured at hydrodynamic center of hydrofoil under consideration in direction parallel to local relative motion and converted to coefficient form by dividing by $\frac{1}{2}\rho_w V^2 S_n$

C_W weight of hydrofoil system converted to coefficient form by dividing by $\frac{1}{2}\rho_w V^2 S$

C_Y side force on hydrofoil system, measured at center of gravity in direction of Y-axis and converted to coefficient form by dividing by $\frac{1}{2}\rho_w V^2 S$

$\left(C_Y\right)_n$ side force on nth hydrofoil, measured at hydrodynamic center of hydrofoil under consideration in direction parallel to Y-axis and converted to coefficient form by dividing by $\frac{1}{2}\rho_w V^2 S_n$

C_Z coefficient of Z-force, with definition similar to that for C_Y

C_l rolling moment about X-axis, converted to coefficient form by dividing by $\frac{1}{2}\rho_w V^2 S b_1$

$\left(C_l\right)_n$ rolling moment at hydrodynamic center of nth hydrofoil about axis parallel to X-axis, converted to coefficient form by dividing by $\frac{1}{2}\rho_w V^2 S_n b_n$

C_m pitching moment about Y-axis, converted to coefficient form by dividing by $\frac{1}{2}\rho_w S c_1$

$\left.\begin{array}{l} C_n \\[2em] \left(C_n\right)_n \end{array}\right\}$ coefficients of yawing moment, with definitions similar to those for C_l and $\left(C_l\right)_n$, respectively

$C_{L_{q_n}}$ the derivative $\partial C_{L_n} \Big/ \partial \dfrac{q c_1}{V}$

x_1 X-component of distance from center of gravity to hydrodynamic center of front hydrofoil, c_1-units

x_2 X-component of distance from hydrodynamic center of rear hydrofoil to center of gravity, c_1-units

l distance between hydrodynamic centers of the two hydrofoils measured parallel to X-axis, c_1-units

z_n Z-component of distance from center of gravity to hydrodynamic center of nth hydrofoil, c_1-units

z_{o_n} operating depth; distance from water surface to hydrodynamic center of nth hydrofoil during steady undisturbed motion, c_n-units

z_o operating depth when depth is same for all hydrofoils in system

r_n parameter of nth hydrofoil used to determine value of $\partial (C_Y)_n \Big/ \partial \left(\dfrac{zb}{V}\right)_n$

y_{c_n} Y-component of distance from hydrodynamic center
          to centroid of lift on one panel of nth hydrofoil,
          b_n-units

z' vertical displacement of center of gravity during
          disturbed motions, c_1-units

z'_n vertical displacement of hydrodynamic center of nth
          hydrofoil during disturbed motions, c_n-units

μ_c mass of hydrofoil system, $\frac{1}{2}\rho_w S c_1$-units

μ_b mass of hydrofoil system, $\frac{1}{2}\rho_w S b_1$-units

K_Y radius of gyration about Y-axis, c_1-units

K_X, K_Z radii of gyration about X- and Z-axes, respectively,
          b_1-units

t time, seconds

s_c time, c_1/V units (To convert nondimensional
          time into second units use $t = s_c c_1/V$. The s_c
          time scale may alternatively be converted into
          distance traversed if values of s_c are multiplied
          by c_1.)

s_b time, b_1/V units

λ stability root, with various numerical subscripts
          used to distinguish the different roots

$Z(t)$ disturbance function; a Z-force of variable magnitude,
          time history of which is indicated by form of
          function (The complete description of any arbitrary
          disturbance acting on the hydrofoil system may be
          expressed by use of this and the additional
          disturbance functions $M(t)$, $Y(t)$, $L(t)$, and
          $N(t)$, with definitions similar to that for $Z(t)$.)

$C_Z(s_c)$ nondimensional disturbance function, similar
          to $Z(t)$ but with force expressed in coefficient
          form and with time in nondimensional units
          (Similar definitions apply to $C_m(s_c)$, $C_Y(s_b)$,
          $C_l(s_b)$, and $C_n(s_b)$.)

α_z, z'_z, θ_z	indicial responses giving motions in α, z', and θ, respectively, caused by sudden application of unit C_Z-disturbance to hydrofoil system
α_m, z'_m, θ_m	indicial responses giving motions in α, z', and θ, respectively, caused by sudden application of unit C_m-disturbance to hydrofoil system
k_1	empirical constant used to determine value of $\partial(C_L)_n/\partial z'_n$
k_2, k_3	empirical constants used to determine value of $\partial(C_L)_n/\partial\alpha_n$
k_4, k_5	empirical constants used to determine value of $\partial(C_D)_n/\partial\alpha_n$

Longitudinal Equations of Motion

The longitudinal motions of the hydrofoil system are referred to the system of axes described in the list of symbols. The choice of axes that correspond to those customarily employed in studies of airplane stability should facilitate extension of the present hydrofoil theory to include the effects of aerodynamic surfaces. The equations of motion are based on the assumption that the hydrofoil system can be replaced by a particle at its center of gravity having a mass m and radii of gyration k_X, k_Y, k_Z about the respective reference axes equal to those of the hydrofoil system. The analysis is also based on the assumption that the velocities V in the direction of motion and u along the X-axis are constant and that departures from the initial conditions of motion are small. The further assumption is made that the longitudinal displacements Z', θ, and along the Z-axis, in the plane of symmetry of the hydrofoil system, are independent of the lateral motions involving the displacements ϕ, ψ, and along the Y-axis. This assumption yields satisfactory theoretical predictions of the motions of airplanes in normal flight and appears warranted, based on the nature of the deviations involved, in the treatment of the longitudinal motion of hydrofoils. Its application to the lateral motions of hydrofoils is made with reservations, as mentioned in the main test.

By the use of D'Alemberts principle, the following equations of equilibrium at the center of gravity are written for the forces and moments involved in the longitudinal motions:

$$
m\frac{d^2Z}{dt^2} - mqV = v\frac{\partial Z}{\partial w} + Z'\frac{\partial Z}{\partial Z'} + \theta\frac{\partial Z}{\partial \theta} + q\frac{\partial Z}{\partial q} + Z(t) \left.\vphantom{\begin{array}{c}1\\1\\1\\1\end{array}}\right\}
$$

$$
mk_Y^2\frac{d^2\theta}{dt^2} = w\frac{\partial M}{\partial w} + Z'\frac{\partial M}{\partial Z'} + \theta\frac{\partial M}{\partial \theta} + q\frac{\partial M}{\partial q} + M(t)
$$

(1)

where $Z(t)$ and $M(t)$ are arbitrary disturbance functions. The equations have the same form as the familiar equations of longitudinal motion for an airplane, except for the addition of derivatives with respect to Z' and θ. The equation of equilibrium involving the X-forces is omitted because u is assumed constant. Equations (1) can be simplified by using $w = \frac{dZ}{dt}$, $\alpha = \frac{w}{V}$, and $q = \frac{d\theta}{dt}$ to give

$$
mV\frac{d\alpha}{dt} - mV\frac{d\theta}{dt} = \alpha\frac{\partial Z}{\partial \alpha} + Z'\frac{\partial Z}{\partial Z'} + \theta\frac{\partial Z}{\partial \theta} + \frac{d\theta}{dt}\frac{\partial Z}{\partial q} + Z(t) \left.\vphantom{\begin{array}{c}1\\1\\1\\1\end{array}}\right\}
$$

$$
mk_Y^2\frac{d^2\theta}{dt^2} = \alpha\frac{\partial M}{\partial \alpha} + Z'\frac{\partial M}{\partial Z'} + \theta\frac{\partial M}{\partial \theta} + \frac{d\theta}{dt}\frac{\partial M}{\partial q} + M(t)
$$

(2)

If equations (2) are rewritten in a nondimensional form, the solutions obtained will be general in character. The method used to make the various terms of the equations nondimensional involves expressing all angles in radians, all forces and moments in the standard NACA coefficient forms

$$
C_Z = \frac{Z}{\frac{1}{2}\rho_w V^2 S}
$$

(3)

$$C_m = \frac{M}{\frac{1}{2}\rho_w V^2 S c_1} \tag{4}$$

all lengths in terms of the chord c_1 of the front hydrofoil, all times in terms of the time c_1/V required for the system to traverse the distance c_1 along the path of motion, and the mass in terms of $\frac{1}{2}\rho_w S c_1$ units. The nondimensional quantities of mass μ_c, time s_c, vertical displacement z', and radius of gyration K_Y about the Y-axis thus bear the following relations to the corresponding dimensional quantities:

$$\mu_c = \frac{m}{\frac{1}{2}\rho_w S c_1} \tag{5}$$

$$s_c = \frac{t}{c_1/V} \tag{6}$$

$$z' = \frac{Z'}{c_1} \tag{7}$$

$$K_Y = \frac{k_Y}{c_1} \tag{8}$$

In equations (3) to (8), ρ_w is the density of water and S is the total projected hydrofoil area in the hydrofoil system.

The nondimensional form of equations (2) becomes

$$\left.
\begin{aligned}
\mu_c \left(\frac{d\alpha}{ds_c} - \frac{d\theta}{ds_c} \right) &= \alpha \frac{\partial C_Z}{\partial \alpha} + z' \frac{\partial C_Z}{\partial z'} + \theta \frac{\partial C_Z}{\partial \theta} + \frac{d\theta}{ds_c} \frac{\partial C_Z}{\partial \frac{qc_1}{V}} + C_Z(s_c) \\
\mu_c K_Y^2 \frac{d^2\theta}{ds_c^2} &= \alpha \frac{\partial C_m}{\partial \alpha} + z' \frac{\partial C_m}{\partial z'} + \theta \frac{\partial C_m}{\partial \theta} + \frac{d\theta}{ds_c} \frac{\partial C_m}{\partial \frac{qc_1}{V}} + C_m(s_c)
\end{aligned}
\right\} \tag{9}$$

Also, from geometric considerations,

$$\frac{dz'}{ds_c} = \alpha - \theta \tag{10}$$

In equations (9), $C_Z(s_c)$ and $C_m(s_c)$ are functions of nondimensional time that describe the application of disturbing force and moment coefficients to the hydrofoil system. The methods used to make the terms of equations (9) nondimensional have the advantage that the nondimensional equations obtained retain the same form as the original force equations; consequently the physical significance of the nondimensional equations should be more readily evident. Solutions of motion obtained from equations (9) are likewise nondimensional and may be considered as proportions, applicable to all similar hydrofoil systems, and capable of conversion to customary engineering units in any given case by use of the characteristic dimensions c_1 and V pertinent to the specific design.

Stable regions and stability roots for the longitudinal motions can be obtained from equations (9) in conjunction with equation (10) by methods discussed in reference 4. The stability equation for the longitudinal motions has the form

$$aD^4 + bD^3 + cD^2 + dD + e = 0 \tag{11}$$

Boundaries for the stable regions were obtained from the conditions

$$(bc - ad)d - b^2e = 0 \tag{12}$$

for the oscillatory boundary and

$$e = 0 \tag{13}$$

for the divergence boundary. The quantities involved in equations (12) and (13) are the coefficients of equation (11), which in turn are functions of the factors of equations (9) and (10). Thus,

$$e = \frac{\partial C_Z}{\partial z'}\left(\frac{\partial C_m}{\partial \theta} + \frac{\partial C_m}{\partial \alpha}\right) - \frac{\partial C_m}{\partial z'}\left(\frac{\partial C_Z}{\partial \theta} + \frac{\partial C_Z}{\partial \alpha}\right) \tag{14}$$

Equation (12) is the familiar Routh's discriminant, but its expression
in terms of the factors in equations (9) and (10) is considered too
lengthy to be presented here.

Longitudinal Derivatives

Values must be assigned to the various partial derivatives
appearing in equations (9) before the equations can be solved. No
experimental values for the derivatives were available; hence computed
values were used. The computed derivatives were evaluated on the
basis of experimental hydrofoil data obtained from results of tests
made in the Langley tank no. 1 at various immersions and speeds.
A discussion of the methods used to compute the various derivatives
follows. Data presented in connection with the discussion are for
hydrofoils of rectangular plan form and tips, with an aspect
ratio of 6, and operating at a velocity of 20 feet per second.
Experimental results indicate that, for a given angle of attack,
marked changes in the lift and drag coefficients of hydrofoils
occur with changes in speed. The values of the derivatives would
undoubtedly be equally affected by any pronounced change in speed
from that assumed in the investigation.

Change in Z-force with vertical displacement of the center of
gravity $\partial C_Z/\partial z'$.— If the center of gravity moves downward, the
hydrofoils are immersed deeper in the water. Experimental results
indicate that an increase in the depth of immersion of a hydrofoil
is accompanied by an increase in the magnitude of the lift obtained.
The increase in lift is proportional to, and of the same sign as,
the initial lift. Thus,

$$\frac{\partial (C_L)_n}{\partial z'_n} = k_1 (C_L)_n \tag{15}$$

Values of k_1 are given in figure 26 for a dihedral angle of 0°
and in figure 27 for dihedral angles of 20° and 30°. The value
of k_1 depends on the normal operating depth z_{o_n} of the hydrofoil.
The discontinuities in the curves of figure 27 coincide with the
point where the tips of the hydrofoil break the surface. In fig-
ure 26 and subsequent figures $(C_L)_n$ is based on the total area
of the hydrofoil instead of the immersed area, and z_{o_n} is
measured in chord lengths of the particular hydrofoil under
consideration.

The value of $\partial C_Z/\partial z'$ for a complete hydrofoil system is the negative sum of the values of $\partial C_{L_n}/\partial z'$ for the individual hydrofoils. The values of $\partial C_{L_n}/\partial z'$ for the various hydrofoils are derived from the $\partial (C_L)_n/\partial z'_n$ values obtained from figures 26 or 27 by making proper allowance for the different areas and chords that are used to make the various terms nondimensional.

Change in Z-force with angle of attack $\partial C_Z/\partial \alpha$.— The value of the derivative $\partial C_Z/\partial \alpha$ is the negative sum of the values of $\partial C_{L_n}/\partial \alpha$ (that is, the slopes of the lift curves) for the individual hydrofoils. As in the case of $\partial C_Z/\partial z'$, differences in the areas used in forming the coefficients must be taken into account when the addition is made. The slope of the lift curve depends on the depth of immersion of the hydrofoil. Typical variations of the slope are given in figure 28 for $0°$ dihedral angle and in figure 29 for various dihedral angles. When figures 28 and 29 are used to determine the slope of the lift curve for the rear hydrofoil, the value obtained is with respect to the local angle of attack α_2 at the rear hydrofoil. In general the value of α_2 is less than that of α (measured at the center of gravity) by the amount of the downwash angle ϵ at the rear hydrofoil. The slope of the lift curve for the rear hydrofoil must be corrected for downwash to give the required slope with respect to α. The correction is applied by multiplying the slope obtained from figure 28 or 29 by the factor $1 - \epsilon_\alpha$, where ϵ_α has some value in the range

$$0 \lessgtr \epsilon_\alpha \lessgtr \frac{2}{A_1} \frac{\partial (C_L)_1}{\partial \alpha_1} \tag{16}$$

In equation (16), A_1 is the aspect ratio of the front hydrofoil and $\partial (C_L)_1/\partial \alpha_1$ is the lift-curve slope obtained from figure 28 or 29 for the front hydrofoil.

Change in Z-force with pitch attitude $\partial C_Z/\partial \theta$.— A change in the pitch attitude of the hydrofoil system will cause a differential change in the depth of immersion of the hydrofoils. The effect on

the Z-force may be estimated from the geometry of the system and the data of figures 26 and 27; thus, for two tandem hydrofoils

$$\frac{\partial C_Z}{\partial \theta} = \frac{S_1}{S} \frac{\partial (C_L)_1}{\partial z'_1} x_1 - \frac{S_2}{S} \frac{c_1}{c_2} \frac{\partial (C_L)_2}{\partial z'_2} x_2 \tag{17}$$

Change in Z-force with pitching velocity $\partial C_Z / \partial \frac{qc_1}{V}$.— The chief effect of a pitching velocity about the center of gravity of the hydrofoil system is to cause a change in local angle of attack at each hydrofoil. The change in effective camber for the pitching hydrofoil introduces a small additional component of vertical force. (See reference 5.) The total effect for two hydrofoils in tandem may be assumed to be

$$\frac{\partial C_Z}{\partial \frac{qc_1}{V}} = -C_{L_{q_1}} - C_{L_{q_2}} \tag{18}$$

where

$$C_{L_{q_1}} = \frac{S_1}{S} \frac{\partial (C_L)_1}{\partial \alpha_1} (-x_1 + 0.5) \tag{19}$$

$$C_{L_{q_2}} = \frac{S_2}{S} \frac{\partial (C_L)_2}{\partial \alpha_2} \left(x_2 - \epsilon_q + 0.5 \frac{c_2}{c_1} \right) \tag{20}$$

In equations (18) and (19), $\partial (C_L)_2 / \partial \alpha_2$ is the lift-curve slope for the rear hydrofoil, based on the local angle of attack α_2; x_1 and

x_2 are the X-components of the locations of the front and rear hydrofoil hydrodynamic centers from the center of gravity expressed in terms of c_1; and ϵ_q indicates the rate of change of downwash angle at the rear hydrofoil with change in nondimensional pitching velocity qc_1/V. The value of ϵ_q will be in the range

$$0 \lesseqgtr \epsilon_q \lesseqgtr \frac{2C_{L_{q_1}}}{\pi A_1} \tag{21}$$

Change in pitching moment with vertical displacement of the center of gravity $\partial C_m/\partial z'$.— The changes in lift, mentioned in the discussion of the change in Z-force with vertical displacement of the center of gravity, produce moment changes about the center of gravity, the magnitude of which depend on the X-components of the distances of the hydrofoil hydrodynamic centers from the center of gravity. The drag also increases with deeper immersion of the hydrofoils. Analysis of the data obtained in Langley tank no. 1 indicates that the change in drag can be expressed as

$$\frac{\partial(C_D)_n}{\partial z'_n} = k_2 (C_L)_n^2 + k_3 \tag{22}$$

Values of k_2 and k_3 are given in figure 30 for 0° dihedral angle and in figure 31 for 30° dihedral angle. The drag changes multiplied by the Z-components of the distances from the center of gravity to the hydrofoil hydrodynamic centers give the drag contributions to the change in pitching moment. For two hydrofoils in tandem

$$\frac{\partial C_m}{\partial z'} = \frac{S_1}{S} \frac{\partial(C_L)_1}{\partial z'_1} x_1 - \frac{S_2}{S} \frac{c_1}{c_2} \frac{\partial(C_L)_2}{\partial z'_2} x_2 - \frac{S_1}{S} \frac{\partial(C_D)_1}{\partial z'_1} z_1 - \frac{S_2}{S} \frac{c_1}{c_2} \frac{\partial(C_D)_2}{\partial z'_2} z_2$$

$$(23)$$

Change in pitching moment with angle of attack $\partial C_m/\partial \alpha$.—
Physical considerations lead to the expression, for two hydrofoils,

$$\frac{\partial C_m}{\partial \alpha} = \frac{S_1}{S} \frac{\partial (C_L)_1}{\partial \alpha_1} x_1 - \frac{S_2}{S} (1 - \epsilon_\alpha) \frac{\partial (C_L)_2}{\partial \alpha_2} x_2 + \frac{S_1}{S} \left[(C_L)_1 - \frac{\partial (C_D)_1}{\partial \alpha_1} \right] z_1$$

$$+ \frac{S_2}{S} (1 - \epsilon_\alpha) \left[(C_L)_2 - \frac{\partial (C_D)_2}{\partial \alpha_2} - \epsilon \frac{\partial (C_L)_2}{\partial \alpha_2} \right] z_2 \qquad (24)$$

where $(C_D)_1$ is the drag coefficient of the front hydrofoil based
on the area of the front hydrofoil; $(C_D)_2$ is the drag coefficient
of the rear hydrofoil based on the area of the rear hydrofoil;
and z_1 and z_2 are the Z-components of the locations of the front-
and rear-hydrofoil hydrodynamic centers from the center of gravity,
expressed in terms of c_1.

The slope of the drag curve for each hydrofoil must be known to
determine $\partial C_m/\partial \alpha$ from equation (24). The empirical relation

$$\frac{\partial (C_D)_n}{\partial \alpha_n} = k_4 (C_L)_n - k_5 \qquad (25)$$

was obtained from an analysis of the experimental data. Values
of k_4 and k_5 varied with the depth of immersion of the
hydrofoils in the manner shown in figure 32 for $0°$ dihedral angle
and in figure 33 for $30°$ dihedral angle.

Change in pitching moment with pitch attitude $\partial C_m/\partial \theta$.— The
differential change in the depth of immersion of the hydrofoils
introduced by a change in the pitch attitude of the hydrofoil
system leads to variations in the lift and drag for each hydrofoil.
These variations can be translated into a variation in pitching
moment about the center of gravity by use of the geometry of the

hydrofoil system and equations (15) and (22). For two tandem hydrofoils

$$\frac{\partial C_m}{\partial \theta} = -\frac{S_1}{S}\frac{\partial\left(C_L\right)_1}{\partial z'_1}x_1{}^2 - \frac{S_2}{S}\frac{c_1}{c_2}\frac{\partial\left(C_L\right)_2}{\partial z'_2}x_2{}^2 + \frac{S_1}{S}\frac{\partial\left(C_D\right)_1}{\partial z'_1}x_1 z_1$$

$$-\frac{S_2}{S}\frac{c_1}{c_2}\frac{\partial\left(C_D\right)_2}{\partial z'_2}x_2 z_2 \tag{26}$$

Change in pitching moment with pitching velocity $\partial C_m \Big/ \partial \frac{qc_1}{V}$.— The only important contribution to the pitching moment produced by a pitching velocity about the center of gravity is that associated with the change in lift on each hydrofoil as a result of the change in local angle of attack. Thus,

$$\frac{\partial C_m}{\partial \dfrac{qc_1}{V}} = -\frac{S_1}{S}\frac{\partial\left(C_L\right)_1}{\partial \alpha_1}x_1{}^2 - \frac{S_2}{S}\left(x_2 - \epsilon_q\right)\frac{\partial\left(C_L\right)_2}{\partial \alpha_2}x_2 \tag{27}$$

Lateral Equations of Motion

Equations expressing the equilibriums of the forces and moments involved in the lateral motions are written on the same assumptions as those used to obtain the longitudinal equations. The equations of lateral motion are

$$m\frac{d^2Y}{dt^2} + mrV = v\frac{\partial Y}{\partial v} + \phi\left(\frac{\partial Y}{\partial \phi} + W\right) + p\frac{\partial Y}{\partial p} + r\frac{\partial Y}{\partial r} + Y(t)$$

$$mk_X{}^2 \frac{d^2\phi}{dt^2} = v\frac{\partial L}{\partial v} + \phi\frac{\partial L}{\partial \phi} + p\frac{\partial L}{\partial p} + r\frac{\partial L}{\partial r} + L(t) \qquad\qquad (28)$$

$$mk_Z{}^2 \frac{d^2\psi}{dt^2} = v\frac{\partial N}{\partial v} + \phi\frac{\partial N}{\partial \phi} + p\frac{\partial N}{\partial p} + r\frac{\partial N}{\partial r} + N(t)$$

where $Y(t)$, $L(t)$, and $N(t)$ are arbitrary disturbance functions. Equations (28) can be simplified by using $v = \frac{dY}{dt}$, $\beta = \frac{Y}{V}$, $p = \frac{d\phi}{dt}$, and $r = \frac{d\psi}{dt}$ to give

$$mV\frac{d\beta}{dt} + mV\frac{d\psi}{dt} = \beta\frac{\partial Y}{\partial \beta} + \phi\left(\frac{\partial Y}{\partial \phi} + W\right) + \frac{d\phi}{dt}\frac{\partial Y}{\partial p} + \frac{d\psi}{dt}\frac{\partial Y}{\partial r} + Y(t)$$

$$mk_X{}^2 \frac{d^2\phi}{dt^2} = \beta\frac{\partial L}{\partial \beta} + \phi\frac{\partial L}{\partial \phi} + \frac{d\phi}{dt}\frac{\partial L}{\partial p} + \frac{d\psi}{dt}\frac{\partial L}{\partial r} + L(t) \qquad\qquad (29)$$

$$mk_Z{}^2 \frac{d^2\psi}{dt^2} = \beta\frac{\partial N}{\partial \beta} + \phi\frac{\partial N}{\partial \phi} + \frac{d\phi}{dt}\frac{\partial N}{\partial p} + \frac{d\psi}{dt}\frac{\partial N}{\partial r} + N(t)$$

Equations (29) will next be written in a nondimensional form similar to that used for the longitudinal equations. Thus, all angles will

be expressed in radians and all forces and moments in the standard NACA coefficient forms

$$C_Y = \frac{Y}{\frac{1}{2}\rho_w V^2 S} \tag{30}$$

$$C_W = \frac{W}{\frac{1}{2}\rho_w V^2 S} \tag{31}$$

$$C_l = \frac{L}{\frac{1}{2}\rho_w V^2 S b_1} \tag{32}$$

$$C_n = \frac{N}{\frac{1}{2}\rho_w V^2 S b_1} \tag{33}$$

Because of the different basis for forming the moment coefficients (cf. equation (4)) in the nondimensional lateral equations of motion, all lengths will be expressed in terms of the span of the front hydrofoil b_1, all values of time in terms of the time b_1/V required for the system to traverse the distance b_1 along the path of motion, and the mass in terms of $\frac{1}{2}\rho_w S b_1$ units. The nondimensional mass μ_b, time s_b, and radii of gyration K_X and K_Z thus bear the following relations to the corresponding dimensional quantities:

$$\mu_b = \frac{m}{\frac{1}{2}\rho_w S b_1} \tag{34}$$

$$s_b = \frac{t}{b_1/V} \tag{35}$$

$$K_X = \frac{k_X}{b_1} \tag{36}$$

$$K_Z = \frac{k_Z}{b_1} \tag{37}$$

The nondimensional form of equations (29) becomes

$$\left.\begin{aligned}
\mu_b\left(\frac{d\beta}{ds_b} + \frac{d\psi}{ds_b}\right) &= \beta\frac{\partial C_Y}{\partial\beta} + \phi\left(\frac{\partial C_Y}{\partial\phi} + C_W\right) + \frac{d\phi}{ds_b}\frac{\partial C_Y}{\partial\frac{pb_1}{V}} + \frac{d\psi}{ds_b}\frac{\partial C_Y}{\partial\frac{rb_1}{V}} + C_Y(s_b) \\
\mu_b K_X^2\frac{d^2\phi}{ds_b^2} &= \beta\frac{\partial C_l}{\partial\beta} + \phi\frac{\partial C_l}{\partial\phi} + \frac{d\phi}{ds_b}\frac{\partial C_l}{\partial\frac{pb_1}{V}} + \frac{d\psi}{ds_b}\frac{\partial C_l}{\partial\frac{rb_1}{V}} + C_l(s_b) \\
\mu_b K_Z^2\frac{d^2\psi}{ds_b^2} &= \beta\frac{\partial C_n}{\partial\beta} + \phi\frac{\partial C_n}{\partial\phi} + \frac{d\phi}{ds_b}\frac{\partial C_n}{\partial\frac{pb_1}{V}} + \frac{d\psi}{ds_b}\frac{\partial C_n}{\partial\frac{rb_1}{V}} + C_n(s_b)
\end{aligned}\right\} \tag{38}$$

where $C_Y(s_b)$, $C_l(s_b)$, and $C_n(s_b)$ are functions of nondimensional time that can be used to define the application of any lateral disturbance to the hydrofoil system.

Lateral Derivatives

In order to obtain a solution from equations (38), the various partial derivatives involved must be given numerical values. No experimentally determined values were available for any of the derivatives, and computed values were therefore used. Experience has shown that theoretical methods are unreliable for obtaining many of the lateral stability derivatives of airplanes. This fact, coupled with the additional complication of the presence of a free surface, suggests that theoretical computations of the derivatives for hydrofoils will be even less satisfactory. Elaborate theoretical analyses to obtain the values of the lateral stability derivatives of hydrofoils, therefore, appear to be unjustified until experimental data are available for use in checking the accuracy of computed values.

For most of the lateral derivatives, the values of the derivatives were first computed with respect to the hydrodynamic center of the hydrofoil for motions at the hydrodynamic center; from the geometry of the hydrofoil system the derivatives at the center of gravity of the hydrofoil system for motions at the center of gravity were obtained. The following discussion will be mainly confined to methods of computing the lateral derivatives at the hydrodynamic center of the hydrofoil. Such derivatives can be readily converted to derivatives at the center of gravity of the hydrofoil system by the use of elementary mechanics when the geometry of the system is known. Numerical data presented in connection with the discussion of the lateral derivatives were obtained from the same sources and the same operating conditions as those used in obtaining the longitudinal derivatives. The expressions derived are for the lateral derivatives of an "ideal" hydrofoil system without supporting struts. The presence of the supporting struts usually required will undoubtedly have a large influence on the values of certain of the lateral derivatives.

Change in Y-force with sideslip $\partial C_Y / \partial \beta$.— During sideslip the effective angle of attack is differentially altered on each side of the hydrofoil, which changes the lift on each half in such a way that a component of side force is introduced. This effect is a function of the dihedral of the hydrofoil. In addition, the direction of the drag force is rotated to one side during sideslipping. The sum of these effects is

$$\frac{\partial \left(C_Y \right)_n}{\partial \beta_n} = - \frac{\partial \left(C_L \right)_n}{\partial \alpha_n} \Gamma_n \tan \Gamma_n - \left(C_D \right)_n \qquad (39)$$

where $(C_Y)_n$ is the coefficient, based on S_n, of the Y-component
of force at the hydrodynamic center of the nth hydrofoil and β_n
is the sideslip angle at the same point. The dihedral angle of
the nth hydrofoil in radians is indicated by Γ_n. The value of
$\dfrac{\partial (C_L)_n}{\partial \alpha_n}$ required in equation (39) can be obtained from figures 28
or 29, and the value of $(C_D)_n$ is given in figure 34 for $0°$ dihedral
angle and in figure 35 for $30°$ dihedral angle.

Change in Y-force with angle of bank $\partial C_Y / \partial \phi$.-- The value of the
derivative $\partial C_Y / \partial \phi$ was estimated by treating each panel separately
as a hydrofoil of which the dihedral angle, angle of attack, centroid
of lift, lift-curve slope, and immersed area vary with angle of bank.
The change in effective aspect ratio, which should be small for small
changes in bank angle, was neglected. The variation in dihedral angle
and immersed area with angle of bank was obtained, by graphical
methods, for banking about the center of gravity of the hydrofoil
system. The changes in lift-curve slope and centroid of lift with
dihedral angle were obtained from figure 36. The value of $\partial (C_L)_n / \partial \alpha_n$
in this figure is for a lift coefficient based on the projected area
of the hydrofoil while banked, rather than on the initial projected
area, and with the lift measured vertically regardless of the bank
attitude. The lateral displacement of the centroid of lift from the
juncture of the hydrofoil panels is given by the value of y_{c_n} in
figure 36. In order to make y_{c_n} nondimensional it is expressed in
terms of twice the projected span of the banked panel. The new angle
of attack of the panel after a change in bank is

$$\alpha = \alpha_0 \cos \Gamma_0 \sec \Gamma \qquad (40)$$

where the subscript 0 refers to the initial values for the hydrofoil
panel, and Γ and α are the values of the dihedral angle and angle
of attack of the panel after a change in bank. (Note that $\Gamma = \Gamma_0 \pm \phi$,
where the sign depends on whether the left or right panel is involved.)
Equation (40) and the values of $\partial (C_L)_n / \partial \alpha_n$ and y_{c_n} obtained from
figure 36 can be used to determine the magnitude and point of
application of C_L for each banked panel. The value of C_Y for
the banked hydrofoil is then determined by rules of simple mechanics.
The value of $\partial C_Y / \partial \phi$ is obtained graphically by plotting the values
of C_Y determined for several values of ϕ and measuring the slope
of the resulting curve.

Change in Y-force with rolling velocity $\partial C_Y / \partial \frac{pb_1}{V}$.— An estimation of the value of the derivative $\partial C_Y / \partial \frac{pb_1}{V}$. was obtained on the assumption that the side force would be zero for rolling of the hydrofoil about its effective center of curvature in front elevation. The derivative for rolling about the center section of the hydrofoil can then be obtained by an expression of the form

$$\frac{\partial (C_Y)_n}{\partial \left(\frac{pb}{V}\right)_n} = r_n \frac{\partial (C_Y)_n}{\partial \beta_n} \tag{41}$$

The parameter r_n is given in figure 37 for various dihedral angles.

Change in Y-force with yawing velocity $\partial C_Y / \partial \frac{rb_1}{V}$.— The derivative $\partial C_Y / \partial \frac{rb_1}{V}$ was assumed to be zero for yawing about the hydrodynamic center of the hydrofoil.

Change in rolling moment with sideslip $\partial C_l / \partial \beta$.— The differential change in lift, produced on each panel of a hydrofoil during sideslip, introduces a component of rolling moment about the center section. An additional component of rolling moment arises because the point of application of the side force produced by sideslip lies above the center section. The sum of these effects is

$$\frac{\partial (C_l)_n}{\beta_n} = y_{c_n} \left(-\frac{\partial (C_L)_n}{\partial \alpha_n} r_n + \frac{\partial (C_Y)_n}{\partial \beta_n} \tan \Gamma_n \right) \tag{42}$$

where y_{c_n} is obtained from figure 36 and $\partial (C_L)_n / \partial \alpha_n$ from figure 29.

Change in rolling moment with angle of bank $\partial C_l / \partial \phi$.— Increments of C_L and C_Y, caused by a change in angle of bank, can be computed by methods outlined in the discussion of $\partial C_Y / \partial \phi$. These increments, when multiplied by appropriate moment arms (expressed in span lengths), are used to obtain a plot of C_l against ϕ, from which the value of $\partial C_l / \partial \phi$ is measured.

Change in rolling moment with rolling velocity $\partial C_l / \partial \frac{pb_1}{V}$.—
Reference 6 gives —0.2 as an average value of the derivative
$\partial C_l / \partial \frac{pb_1}{V}$ for a conventional airplane wing. The value for a hydro-
foil will probably be somewhat smaller, but in the absence of
experimental data the average value mentioned was used for rolling
of the hydrofoil about its center section.

Change in rolling moment with yawing velocity $\partial C_l / \partial \frac{rb_1}{V}$.— The
average value

$$\frac{\partial (C_l)_n}{\partial \left(\frac{rb}{V}\right)_n} = \frac{(C_L)_n}{8} \tag{43}$$

was used for the derivative $\partial C_l / \partial \frac{rb_1}{V}$. Reference 6 indicates that
this value is suitable for wings with moderate taper, and the loss
of lift on parts of a hydrofoil that approach the surface would
result in a similar lift distribution if the hydrofoil had dihedral.

Change in yawing moment with sideslip $\partial C_n / \partial \beta$.— During sideslip
the lift vector for each panel of a hydrofoil remains perpendicular
to both the hydrofoil leading edge and the direction of motion.
Hence, the projection of the lift vector on the horizontal plane
rotates forward for the leading panel and rearward for the trailing
panel. The resulting couple about the hydrodynamic center of the
hydrofoil is

$$\frac{\partial (C_n)_n}{\partial \beta_n} = -(C_L)_n \, y_{c_n} \, \tan \Gamma_n \tag{44}$$

Change in yawing moment with angle of bank $\partial C_n / \partial \phi$.— If, during
banked motion of a hydrofoil, the centroid of drag for each panel is
assumed to have the same location as the centroid of lift and if the
additional assumption is made that the variation of drag with lift is
the same in the banked attitude as for zero bank, $\partial C_n / \partial \phi$ can be
computed by methods similar to those used for $\partial C_Y / \partial \phi$ and $\partial C_l / \partial \phi$.

Change in yawing moment with rolling velocity $\partial C_n / \partial \frac{pb_1}{V}$.— The average value given in reference 6 for an elliptical distribution of lift was used for the derivative $\partial C_n / \partial \frac{pb_1}{V}$. Thus

$$\frac{\partial \left(C_n\right)_n}{\partial \left(\frac{pb}{V}\right)_n} = -\frac{\left(C_L\right)_n - \frac{\partial \left(C_D\right)_n}{\partial \alpha_n}}{16} \tag{45}$$

The elliptical loading was assumed to approximate the loss in lift over the tip parts of a hydrofoil with dihedral and with the tips at the water surface.

Change in yawing moment with yawing velocity $\partial C_n / \partial \frac{rb_1}{V}$.— The value

$$\frac{\partial \left(C_n\right)_n}{\partial \left(\frac{rb}{V}\right)_n} = -\frac{\left(C_D\right)_n}{8} \tag{46}$$

appears to be a suitable approximation to the expression given by Glauert for elliptical wings (see reference 6) and hence was used in the calculations. The selection of elliptical loading was based on the same considerations as for the derivative $\partial C_n / \partial \frac{pb_1}{V}$.

REFERENCES

1. Tietjens, O.; Das Tragflächenboot. Werft Reederei Hafen,
    Jahrg. 18, Heft 7, April 1, 1937, pp. 87-90; Heft 8,
    April 10, 1937, pp. 106-109.

2. Guidoni, A.; Seaplanes — Fifteen Years of Naval Aviation.
    Jour. R.A.S., vol. XXXII, no. 205, Jan. 1928, pp. 25-64.

3. Jones, B. Melvill; Dynamics of the Airplane. The Equations
    of Motion with Solutions for Small Disturbances from Steady
    Symmetric Flight. Vol. V of Aerodynamic Theory, div. N,
    ch. V, secs. 6-17, W. F. Durand, ed., Julius Springer (Berlin),
    1935, pp. 124-130.

4. Imlay, Frederick H.; A Theoretical Study of Lateral Stability
    with an Automatic Pilot. NACA Rep. No. 693, 1940.

5. Glauert, H.; The Lift and Pitching Moment of an Aerofoil Due
    to a Uniform Angular Velocity of Pitch. R. & M. No. 1216,
    British A.R.C., 1929.

6. Zimmerman, Charles H.; An Analysis of Lateral Stability in
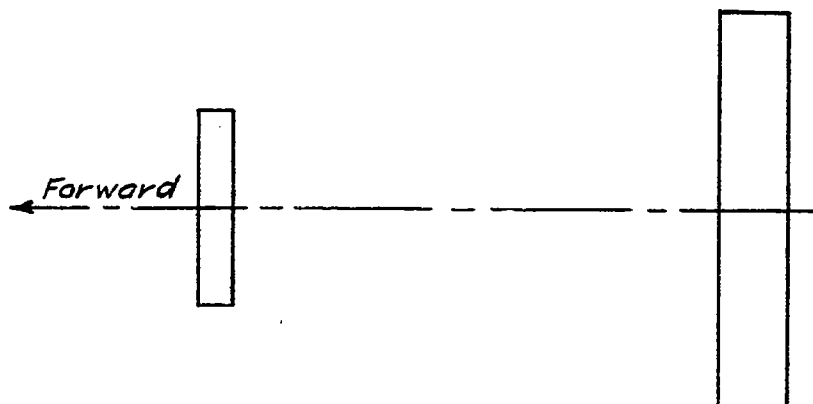   Power-Off Flight with Charts for Use in Design. NACA
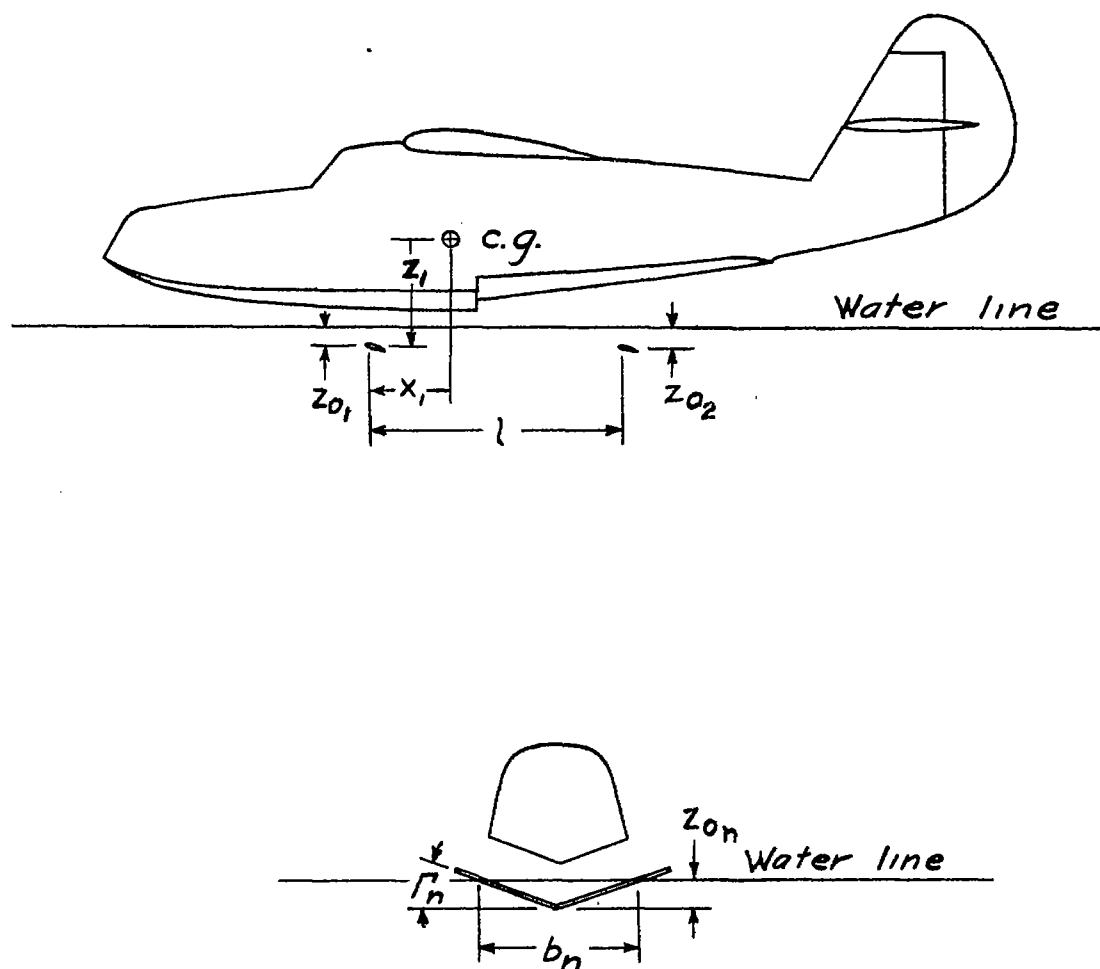   Rep. No. 589, 1937.
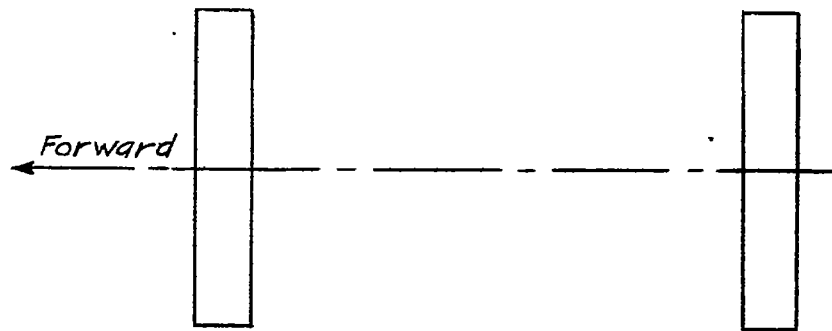
Arrangement 1
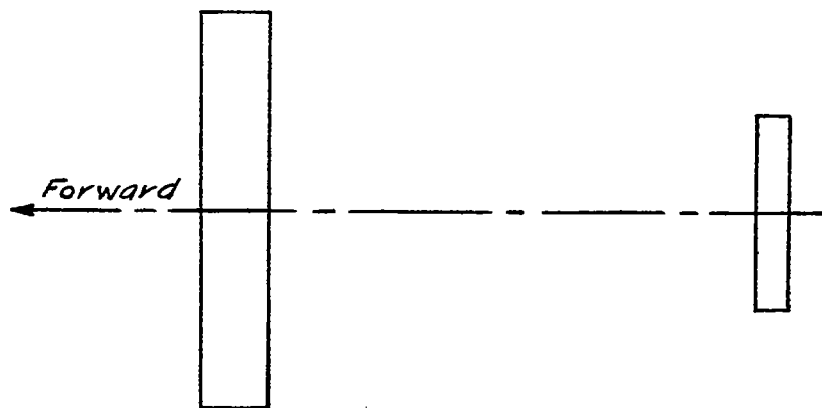
Arrangement 2

Arrangement 3

Figure 1.- Hydrofoil plan-form arrangements assumed

Fig. 2   NACA TN No. 1285

Figure 2.— Definition of symbols for a representative hydrofoil system.
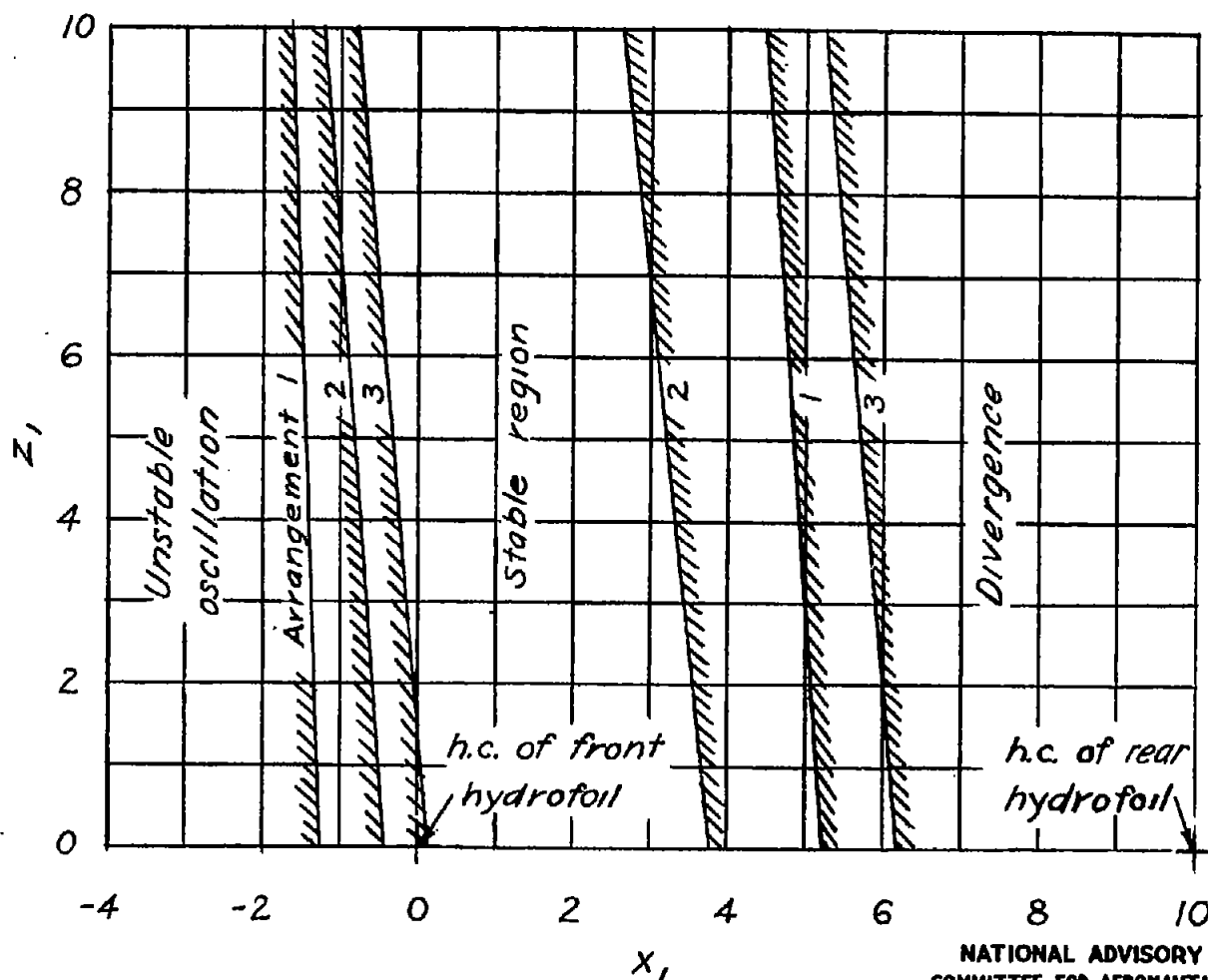
Figure 3.- Stable regions for three area distributions. $\Gamma = 0°$; $\epsilon = 0$; $l = 10.0 c_1$; $z_0 = 1.00 c_1$; $K_Y = 6.67 c_1$. (For this figure c_1 is the chord for arrangement 1, in which the two hydrofoils are identical.)
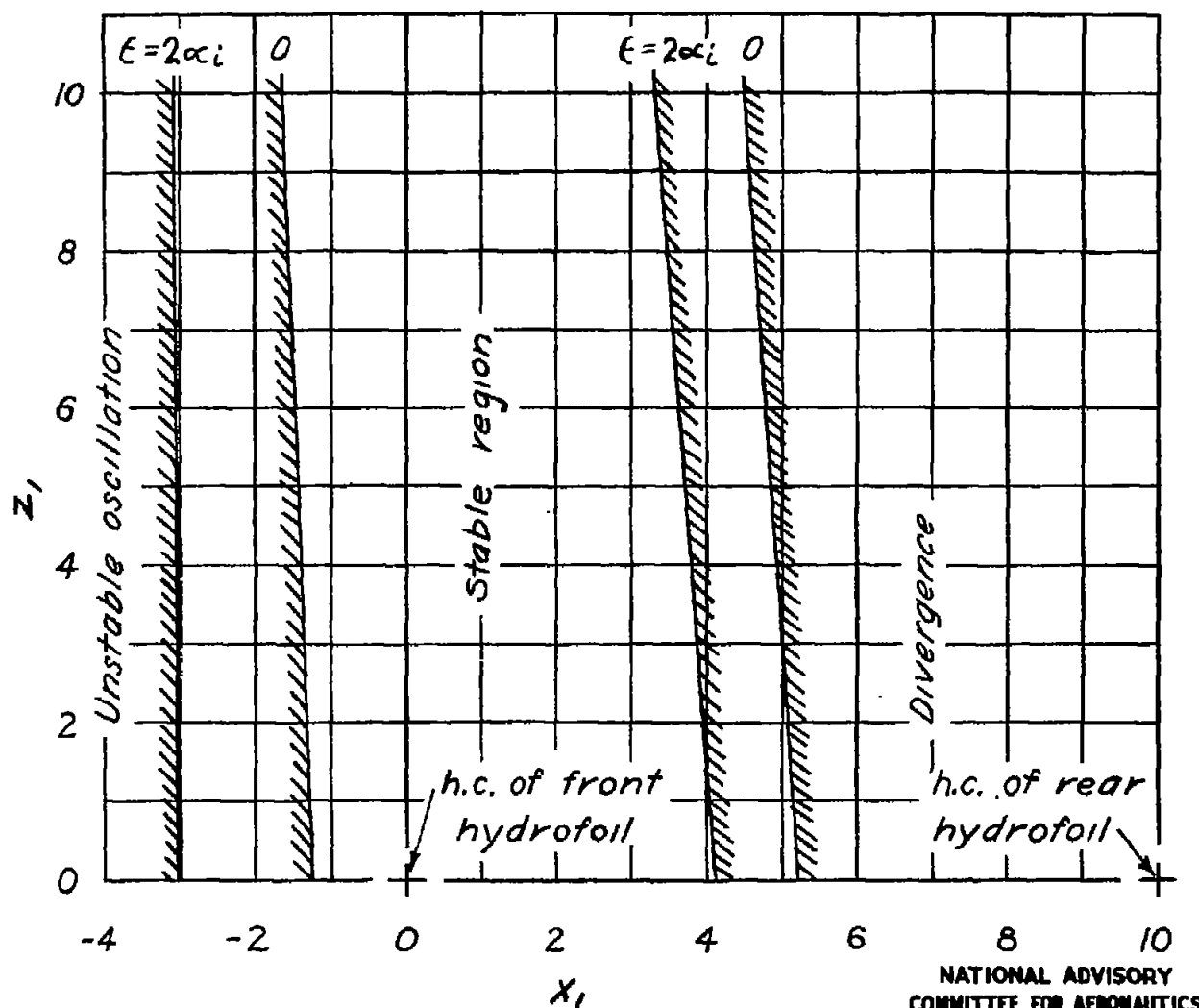
Fig. 3

Figure 4.- Stable regions for two downwash angles. $\Gamma = 0°$; $S_2 = S_1$; $l = 10.0 c_1$; $z_0 = 1.00 c_1$; $K_Y = 6.67 c_1$.
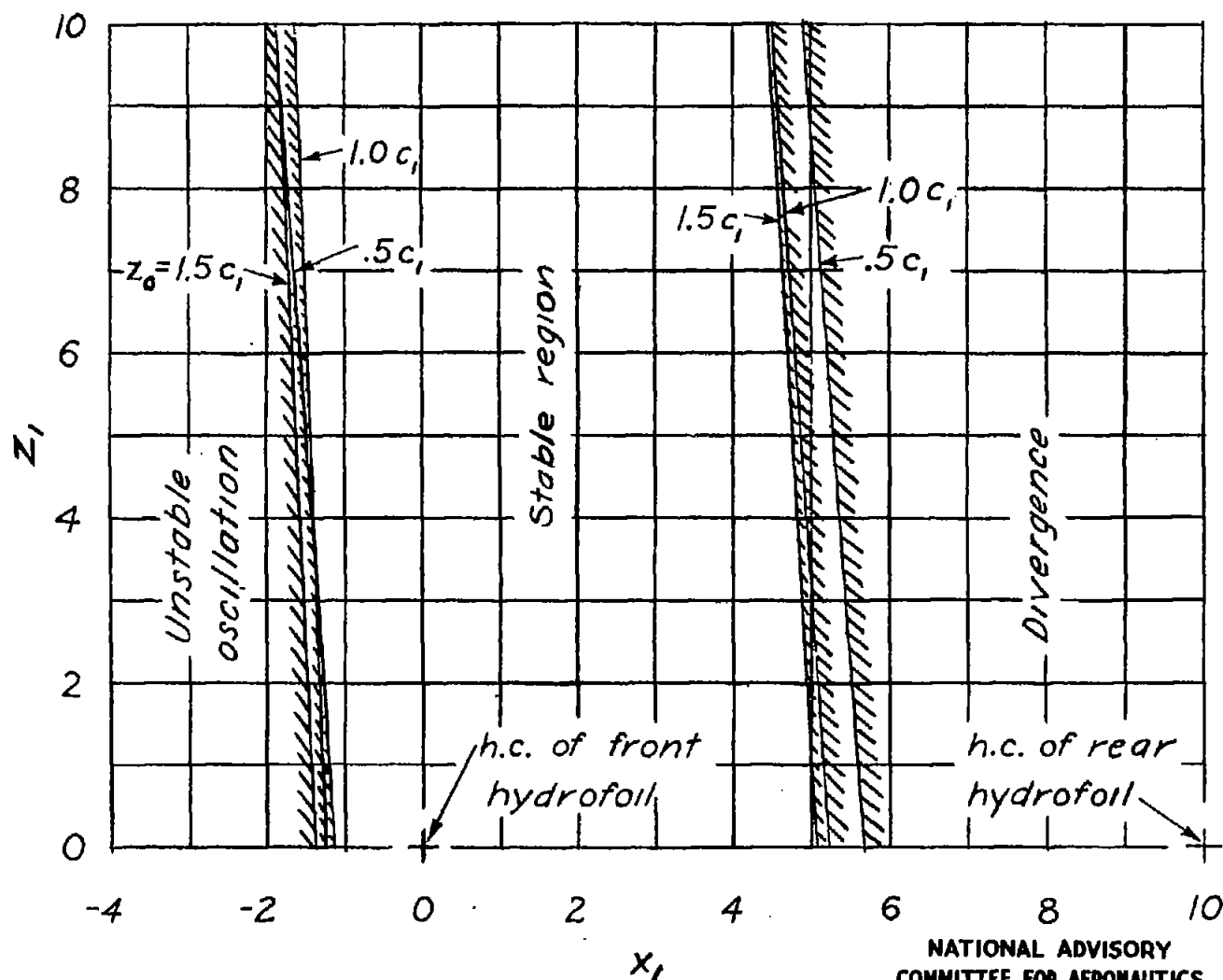
Fig. 4

Fig. 5

Figure 5.- Stable regions for three immersion depths.
$\Gamma = 0°$; $S_2 = S_1$; $\epsilon = 0$; $l = 10.0 c_1$; $K_Y = 6.67 c_1$.
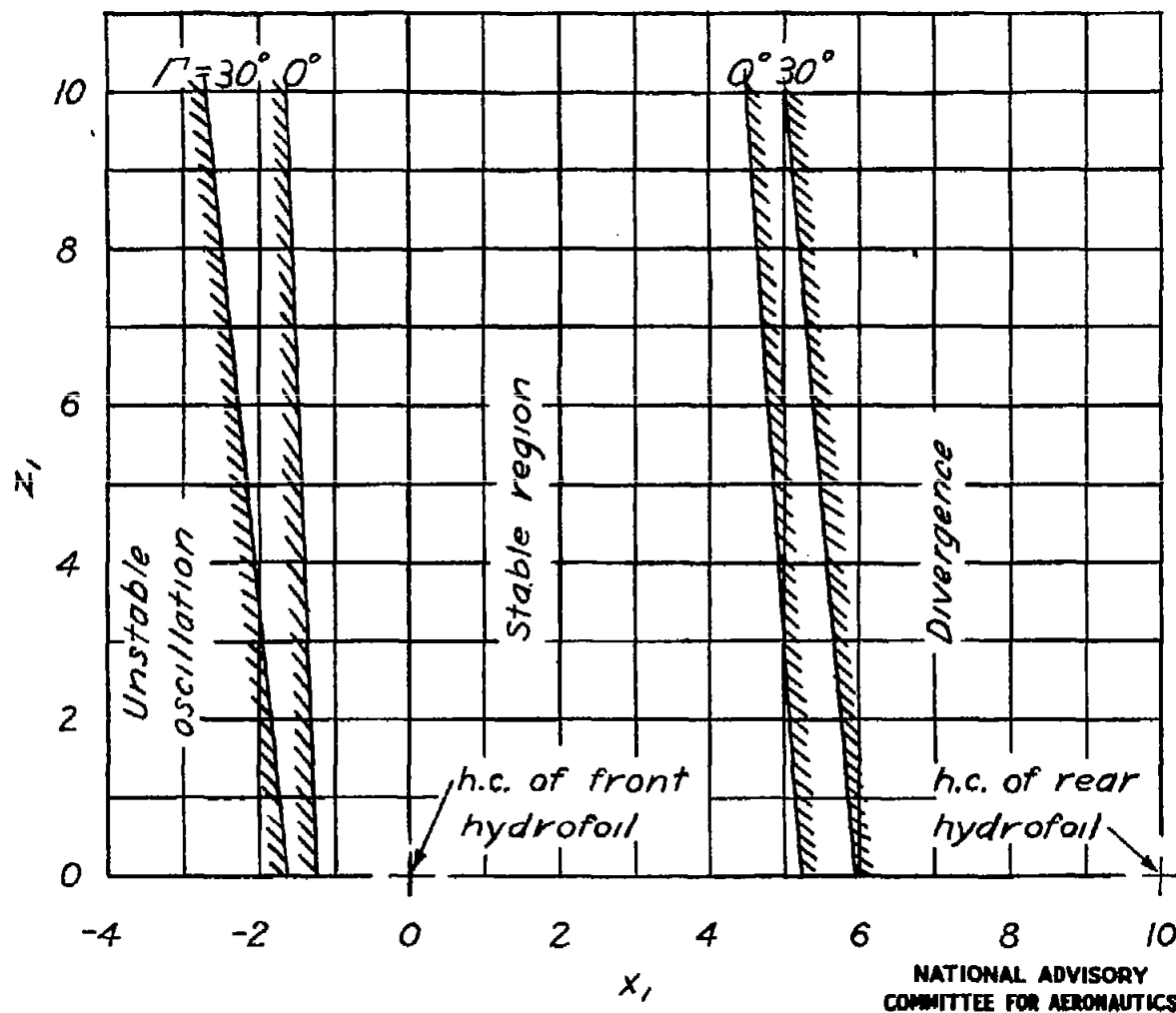
NATIONAL ADVISORY
COMMITTEE FOR AERONAUTICS

Fig. 6

Figure 6.- Stable regions for two dihedral angles. $S_z = S_1$; $\epsilon = 0$; $l = 10.0 c_1$; $z_0 = 1.00 c_1$ for $\Gamma = 0^\circ$, and $1.74 c_1$ for $\Gamma = 30^\circ$; $K_Y = 6.67 c_1$.
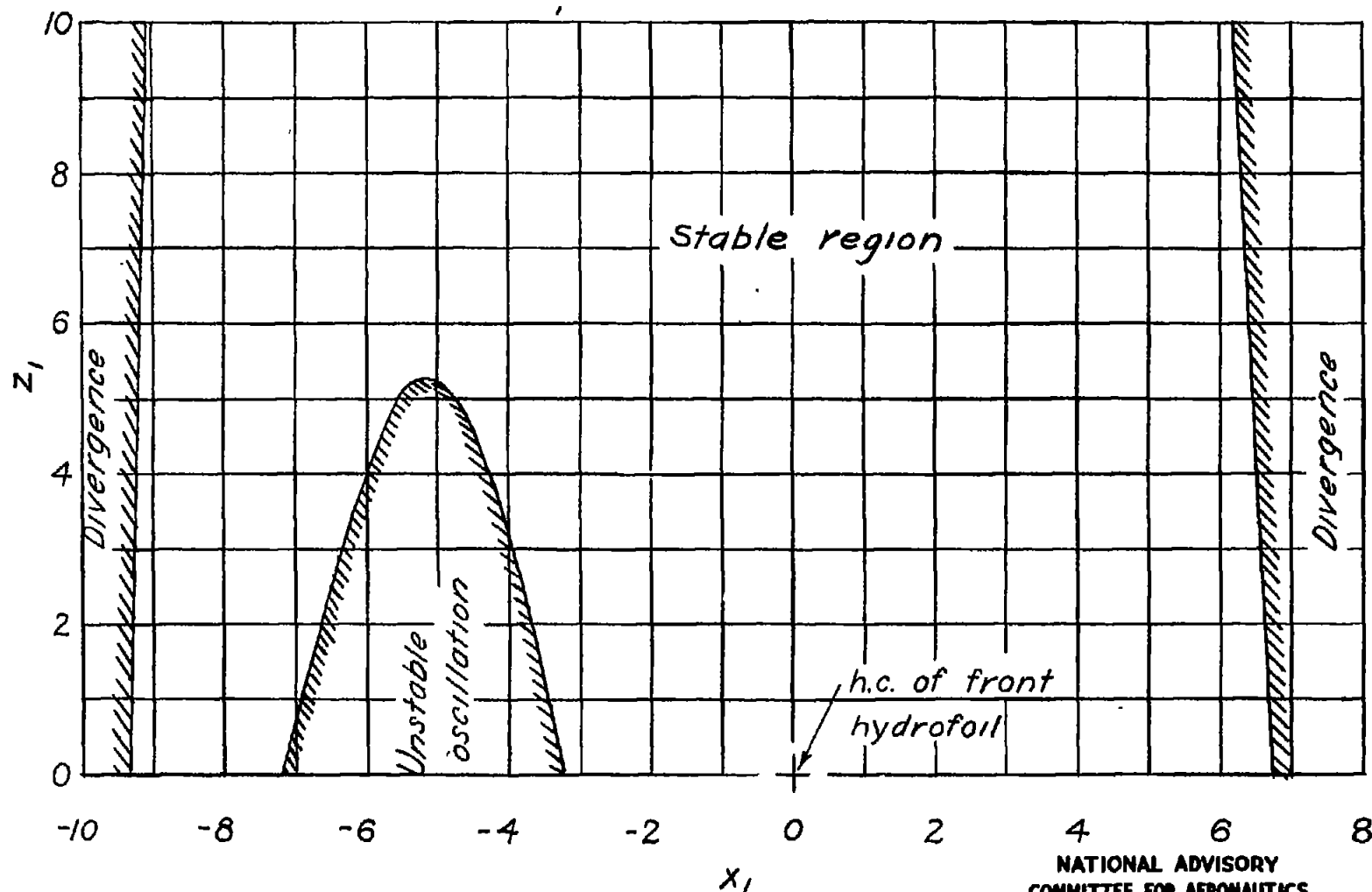
Figure 7.- Stable region with $\partial C_L / \partial z'$ double that for $\Gamma = 30°$. $S_2 = S_1$; $\epsilon = 0$; $l = 10.0 c_1$; $K_Y = 6.67 c_1$.

Fig. 7

Fig. 8

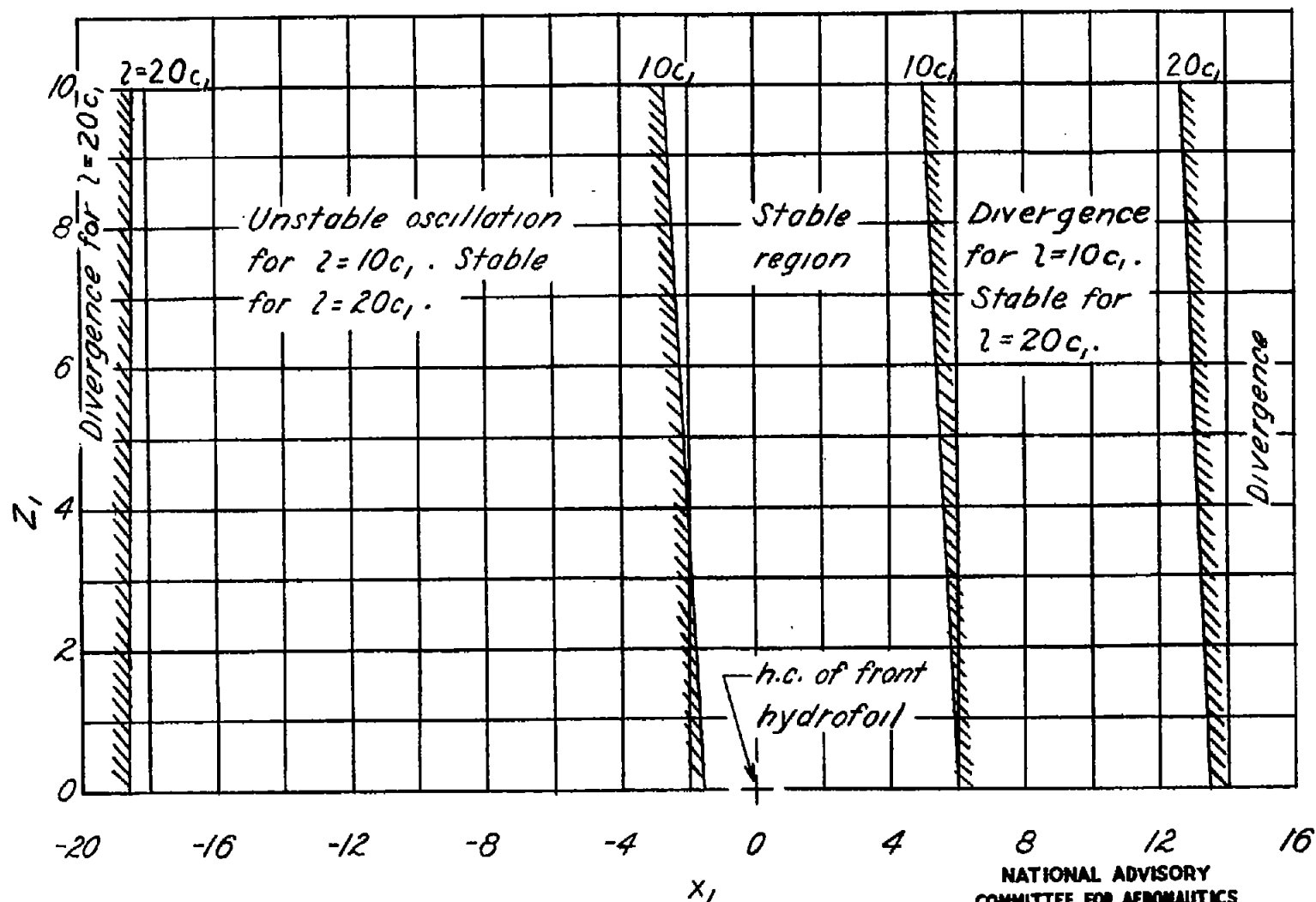Figure 8.- Stable regions for two longitudinal spacings. $\Gamma = 30°$; $S_2 = S_1$; $\epsilon = 0$; $z_o = 1.74c_1$; $K_y = 6.67c_1$.
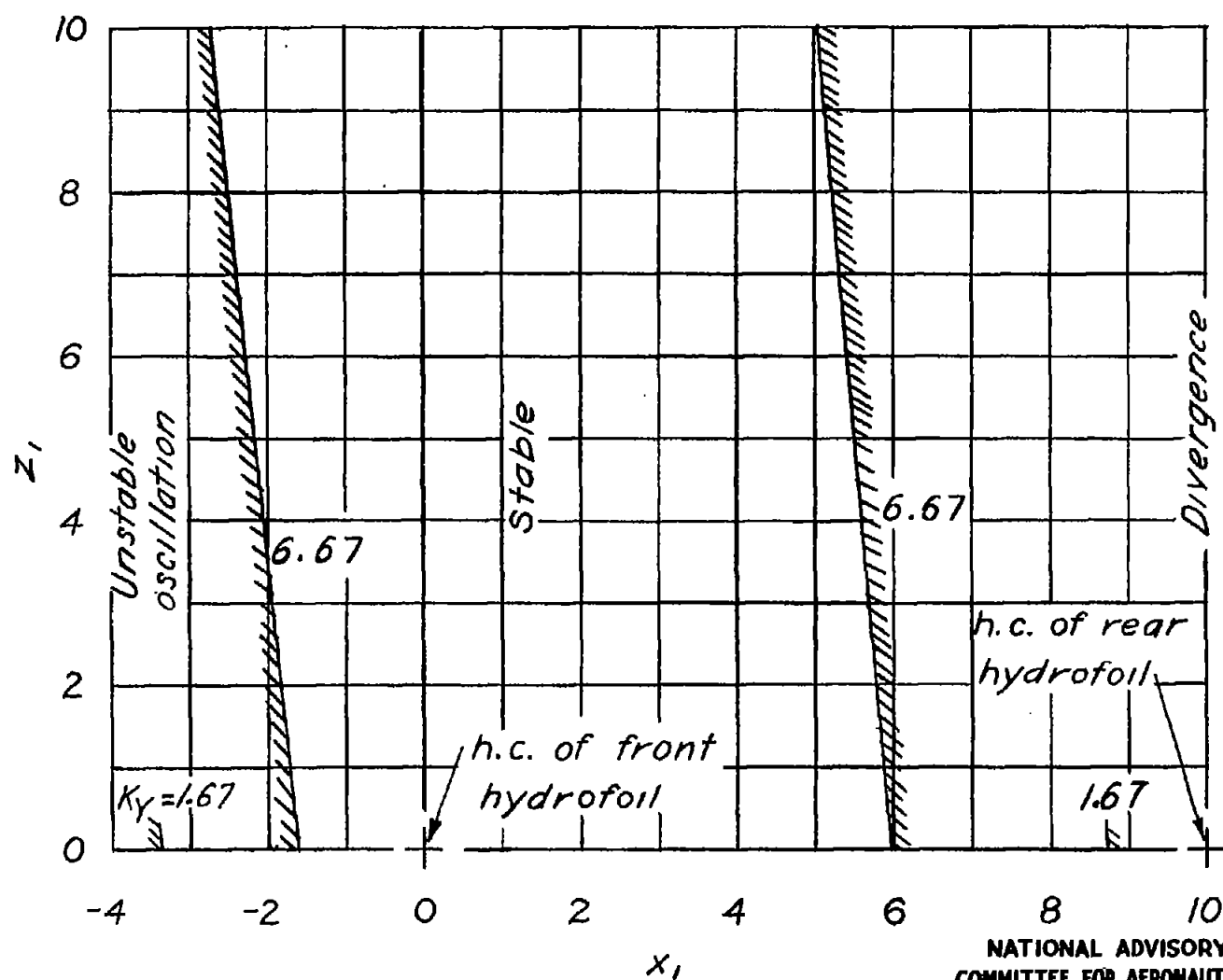
Figure 9.- Range of stable center-of-gravity location for two values of K_Y. $\Gamma = 30°$; $S_2 = S_1$; $\epsilon = 0$; $l = 10.0 \, c_1$; $z_0 = 1.74 \, c_1$.

Fig. 9

Fig. 10   NACA TN No. 1285

Figure 10.- Variation of real parts of stability roots with x_1. $\Gamma = 30°$; $S_2 = S_1$; $\epsilon = 0$; $l = 10.0\,c_1$; $z_0 = 1.74\,c_1$; $K_y = 6.67\,c_1$; $z_1 = 5.00\,c_1$.

Figure 11.- Variation of real parts of
     stability roots with x_l. $\Gamma = 30°$;
$S_2 = S_1$; $\epsilon = 2\alpha_i$; $l = 10.0 c_l$; $z_0 = 1.74 c_l$;
$K_Y = 6.67 c_l$; $z_l = 5.00 c_l$.

Fig. 12   NACA TN No. 1285

Figure 12.- Variation of real parts of stability roots with x_i. $\Gamma = 0°$; $S_z = S_i$; $\epsilon = 0$; $l = 10.0 c_i$; $z_o = 1.00 c_i$; $K_y = 6.67 c_i$; $z_i = 5.00 c_i$.
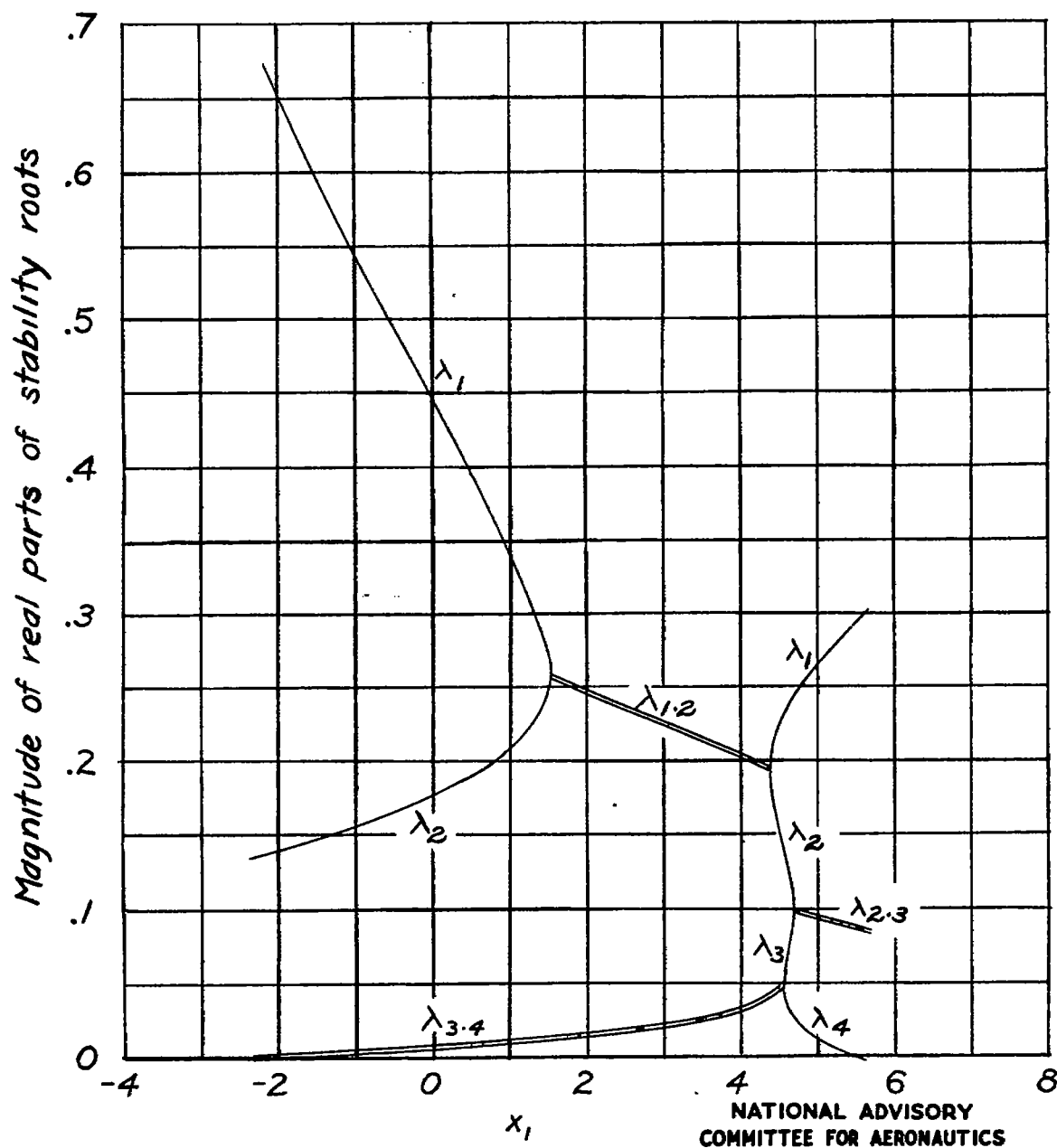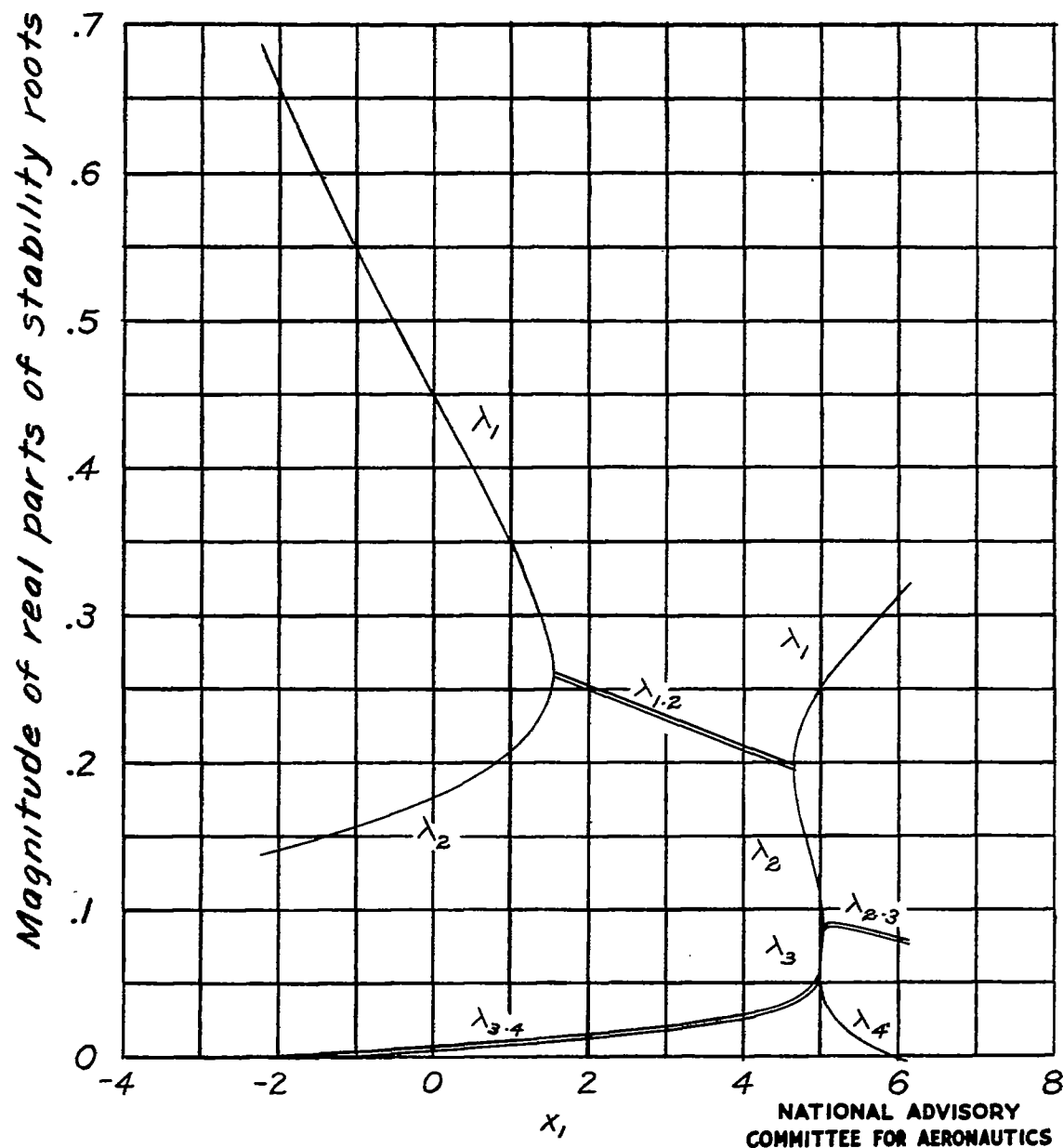
Figure 13.- Variation of real parts of stability roots with x_i. $\Gamma = 30°$; $S_2 = S_i$; $\epsilon = 0$; $l = 10.0 c_i$; $z_0 = 1.74 c_i$; $K_Y = 6.67 c_i$; $z_i = 0$.

Axis labels: Magnitude of real parts of stability roots; x_i

Curve labels: λ_i, $\lambda_{1\cdot2}$, λ_2, $\lambda_{2\cdot3}$, λ_3, $\lambda_{3\cdot4}$, λ_4

NATIONAL ADVISORY
COMMITTEE FOR AERONAUTICS

Fig. 14   NACA TN No. 1285

Figure 14.— Variation of real parts of stability roots with x_i. $\Gamma = 30°$; $S_2 = S_i$; $\epsilon = 0$; $l = 10.0 c_i$; $z_0 = 1.74 c_i$; $K_y = 6.67 c_i$; $z_i = 10.00 c_i$.

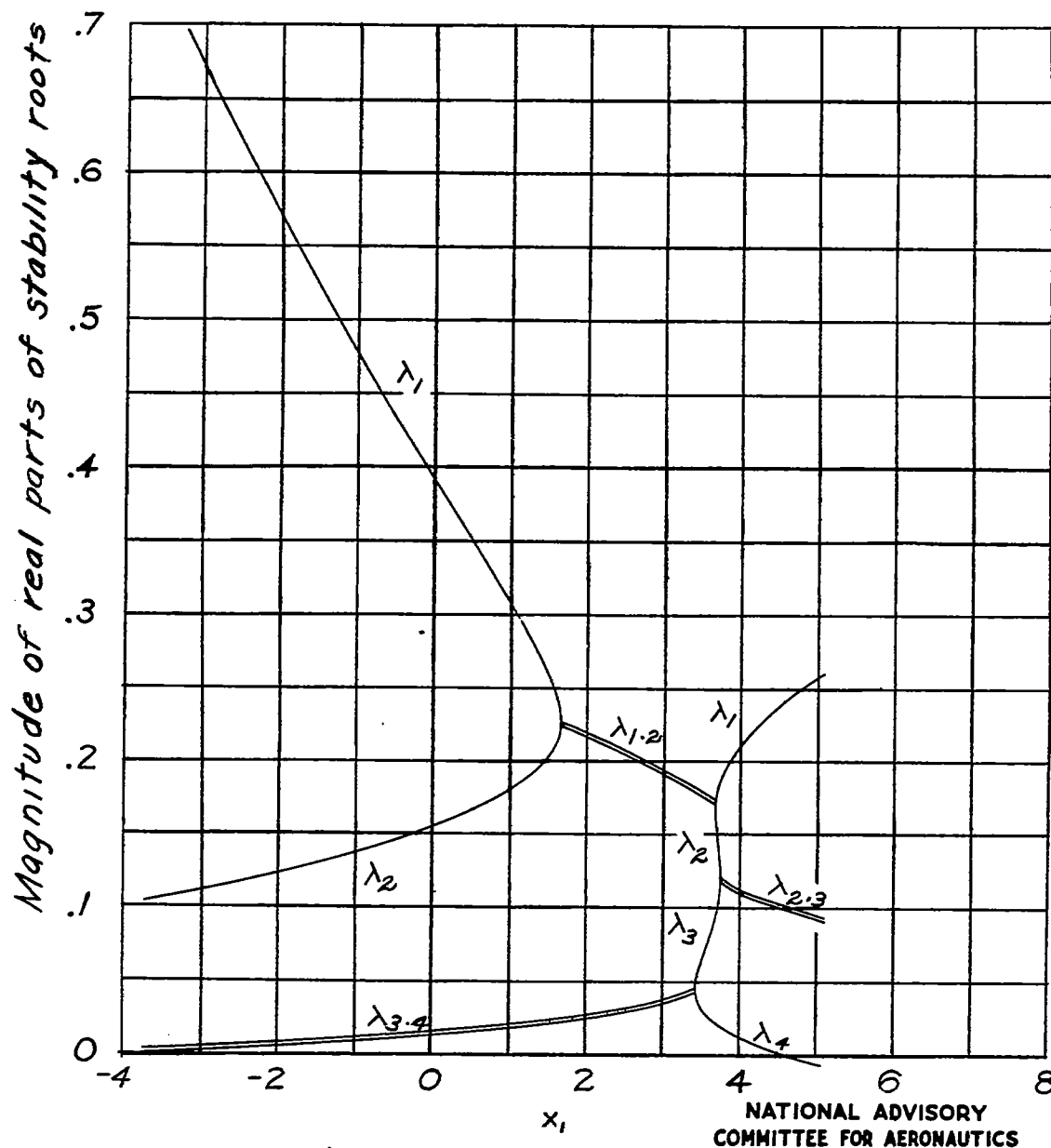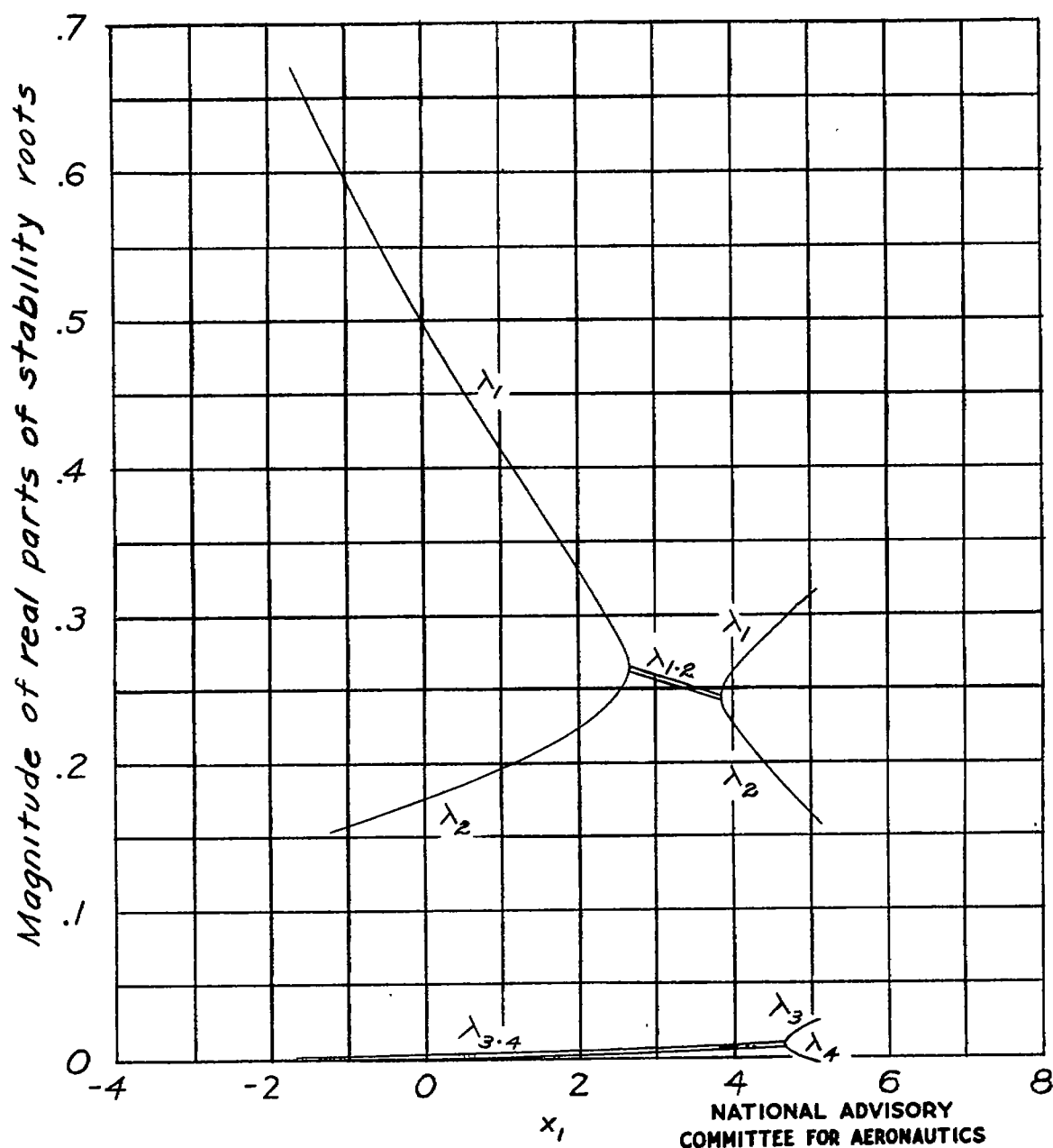Figure 15.- Variation of real parts of
stability roots with x_1 for increased
vertical damping. $S_2 = S_1$; $\epsilon = 0$;
$l = 10.0 c_1$; $K_Y = 6.67 c_1$; $z_1 = 5.00 c_1$.

Fig. 16　　　　　　　　　　　　　　　　　　　NACA TN No. 1285
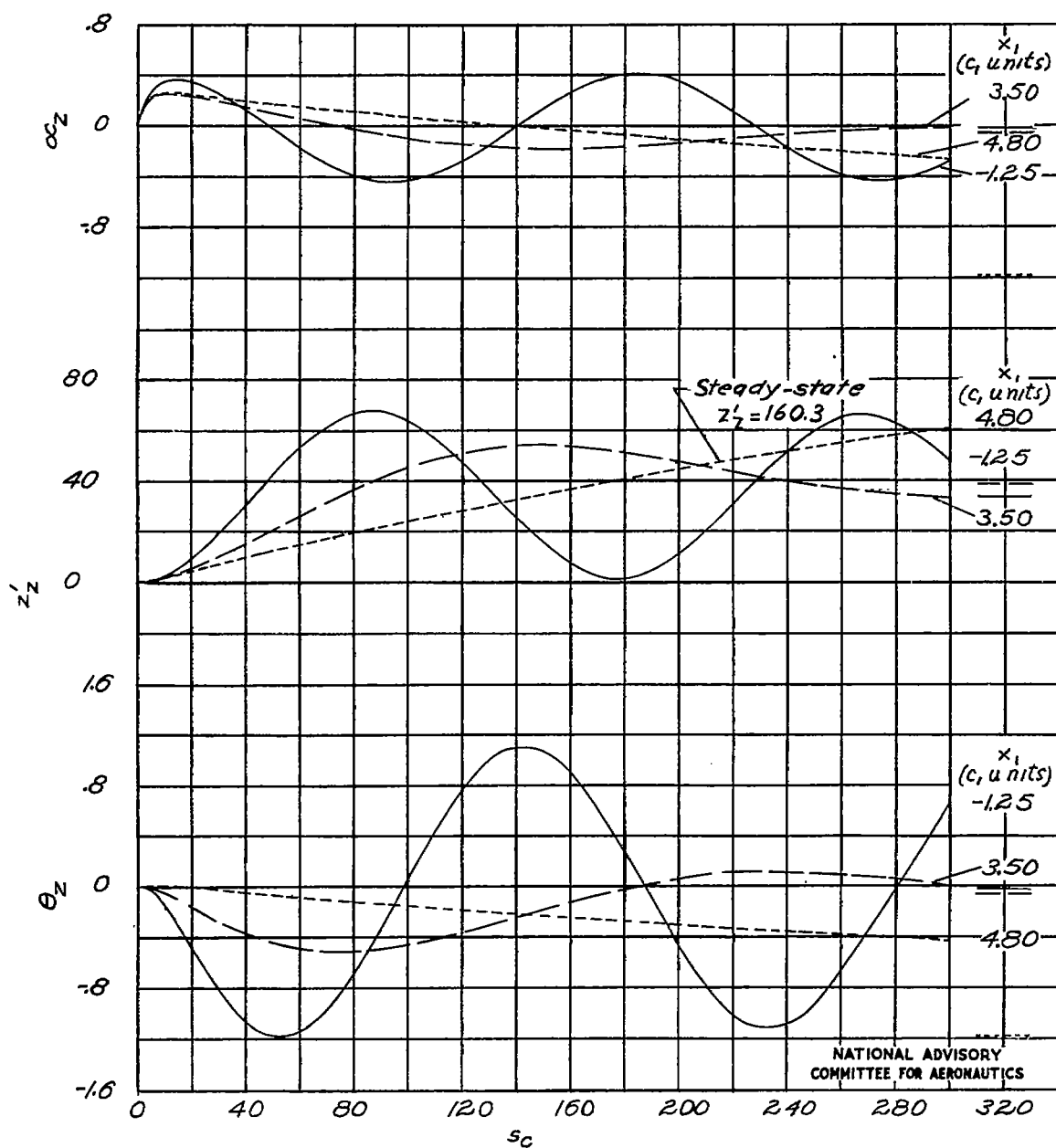
Figure 16.- Indicial responses for unit C_Z disturbance. $\Gamma = 0^\circ$; $S_a = S_1$; $\epsilon = 0$; $l = 10.0 c_1$; $z_0 = 1.00 c_1$; $K_Y = 6.67 c_1$; $z_1 = 5.00 c_1$; $x_1 = -1.25 c_1$, $3.50 c_1$, or $4.80 c_1$.
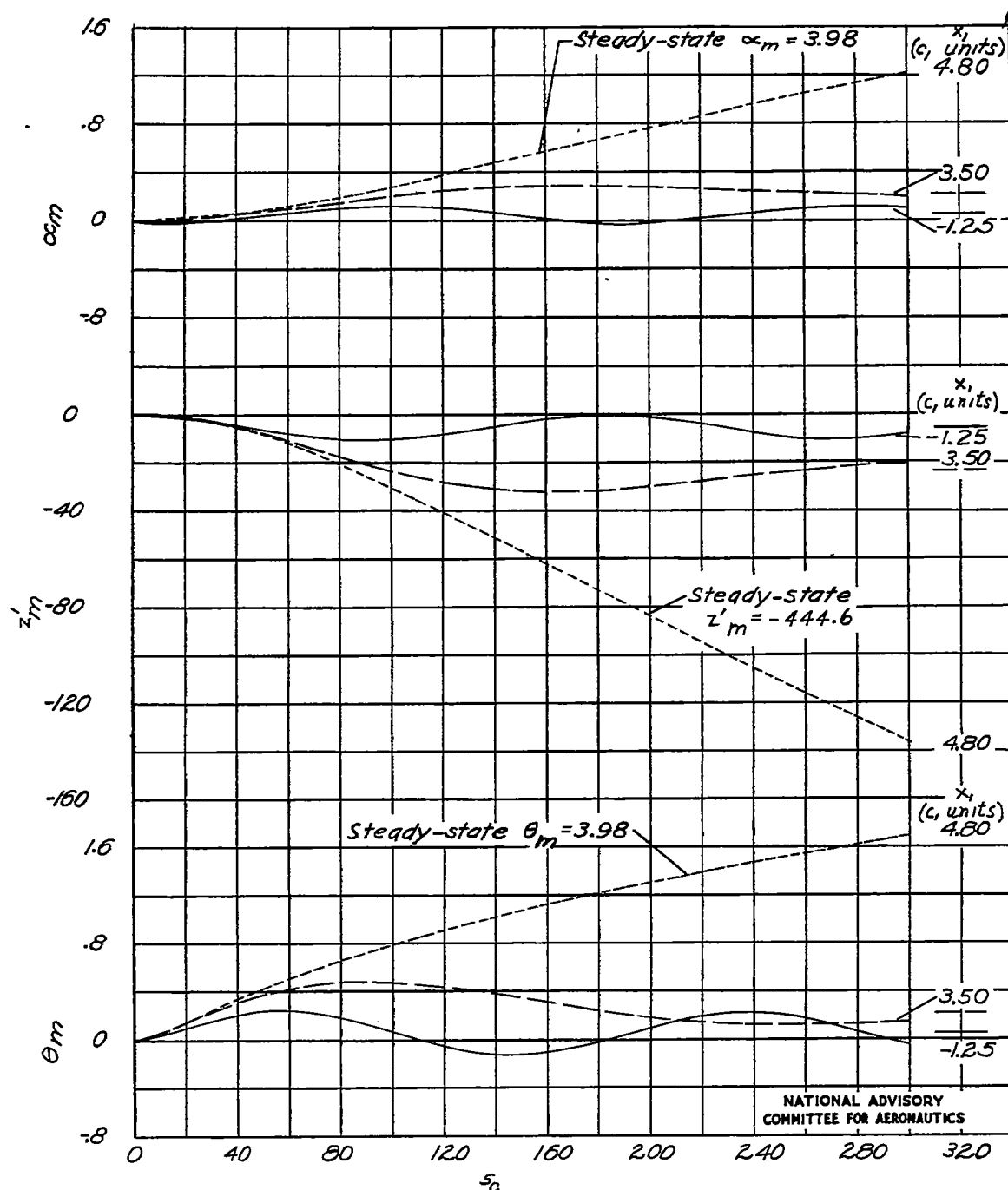
Figure 17.— Indicial responses for unit C_m disturbance. $\Gamma = 0°$;
$S_2 = S_1$; $\epsilon = 0$; $l = 10.0c_1$; $z_0 = 1.00c_1$; $K_Y = 6.67c_1$; $z_1 = 5.00c_1$;　$x_1 = -1.25c_1$,
$3.50c_1$, or $4.80c_1$.

Fig. 18   NACA TN No. 1285
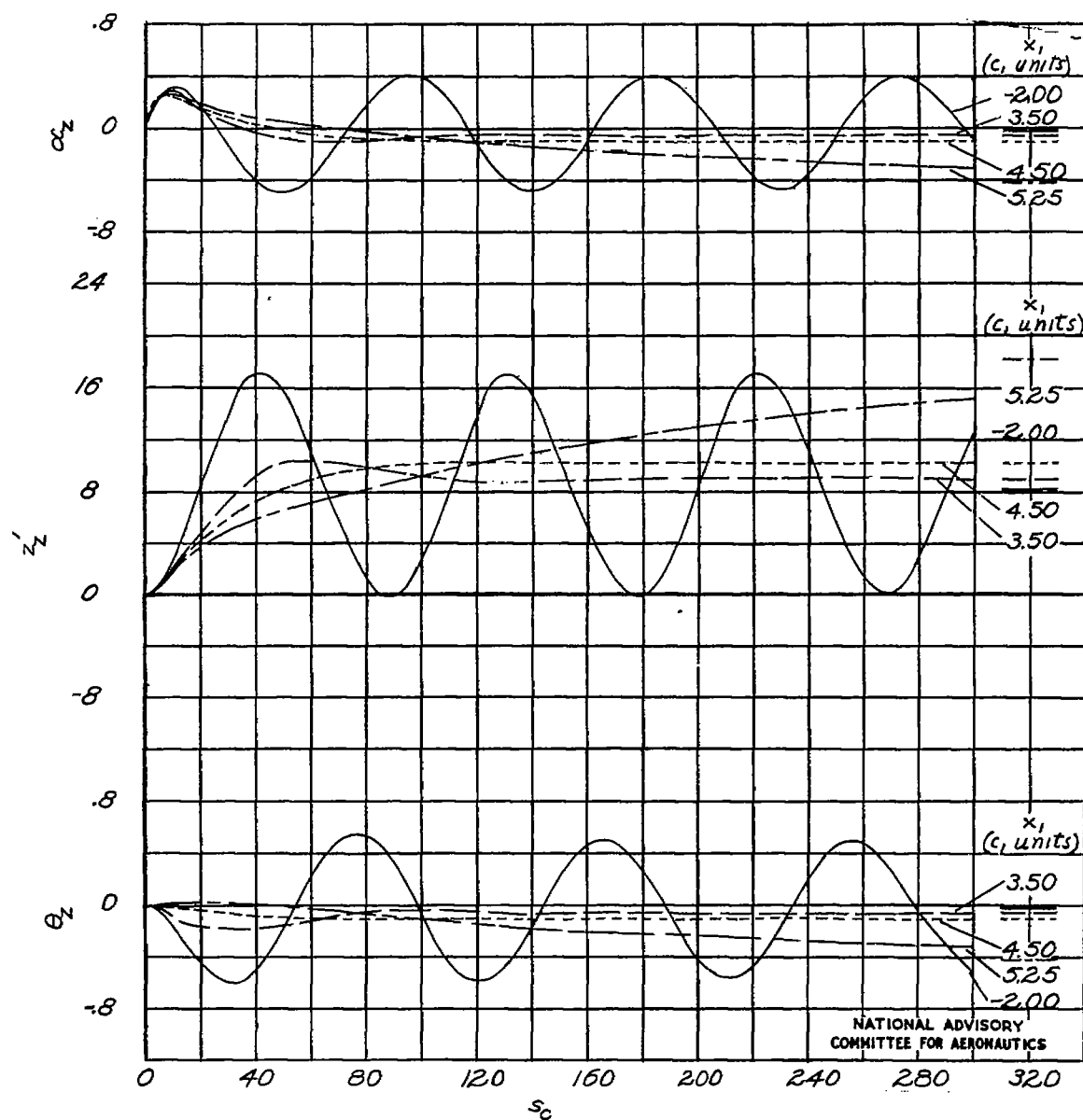
Figure 18.— Indicial responses for unit C_Z disturbance. $\Gamma = 30°$; $S_2 = S_1$;
$\epsilon = 0$; $l = 10.0c_1$; $z_o = 1.74c_1$; $K_y = 6.67c_1$; $z_1 = 5.00c_1$; $x_1 = -2.00c_1$,
3.50c_1, 4.50c_1, or 5.25c_1.
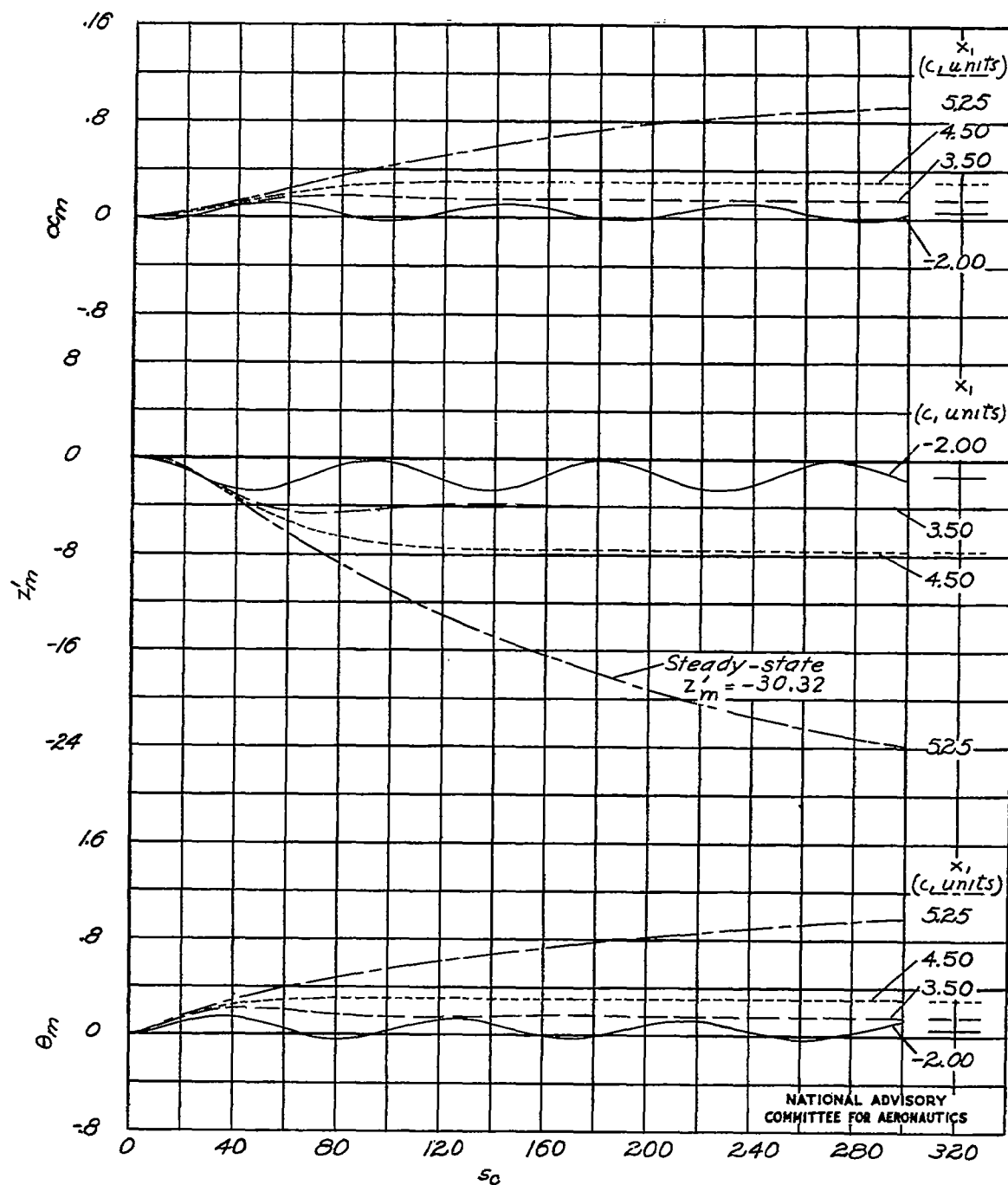
Figure 19.- Indicial responses for unit C_m disturbance. $\Gamma = 30°$; $S_2 = S_1$; $\epsilon = 0$; $l = 10.0c_1$; $z_o = 1.74c_1$; $K_Y = 6.67c_1$; $z_1 = 5.00c_1$; $x_1 = -2.00c_1$, $3.50c_1$, $4.50c_1$, or $5.25c_1$.

Fig. 20   NACA TN No. 1285
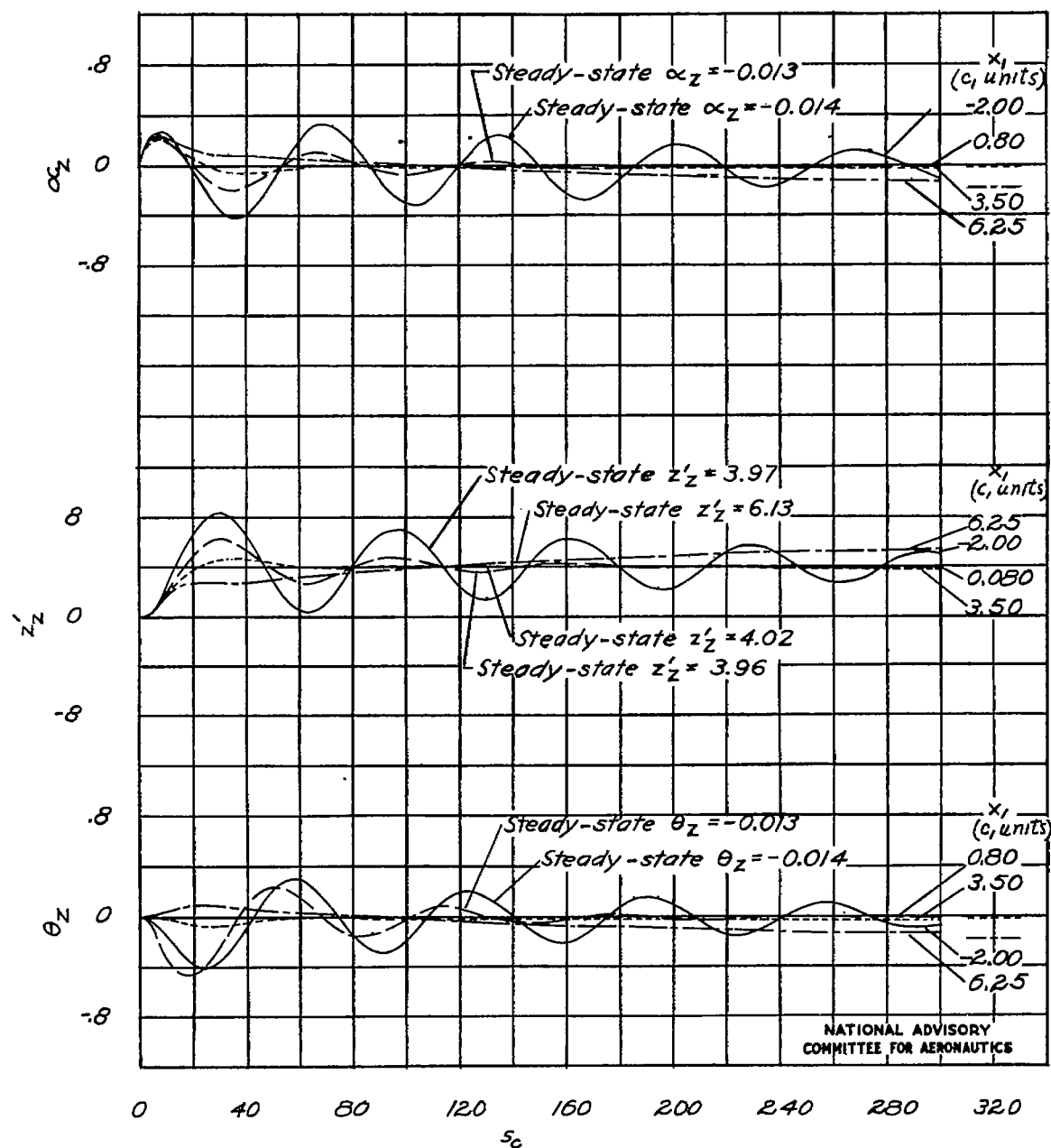
Figure 20.- Indicial responses for unit C_Z disturbance. $\partial C_L/\partial z'$ double that for $\Gamma = 30°$; $S_2 = S_1$; $\epsilon = 0$; $l = 10.0 c_1$; $K_Y = 6.67 c_1$; $z_1 = 5.00 c_1$; $x_1 = -2.00 c_1$, $0.80 c_1$, $3.50 c_1$, or $6.25 c_1$.
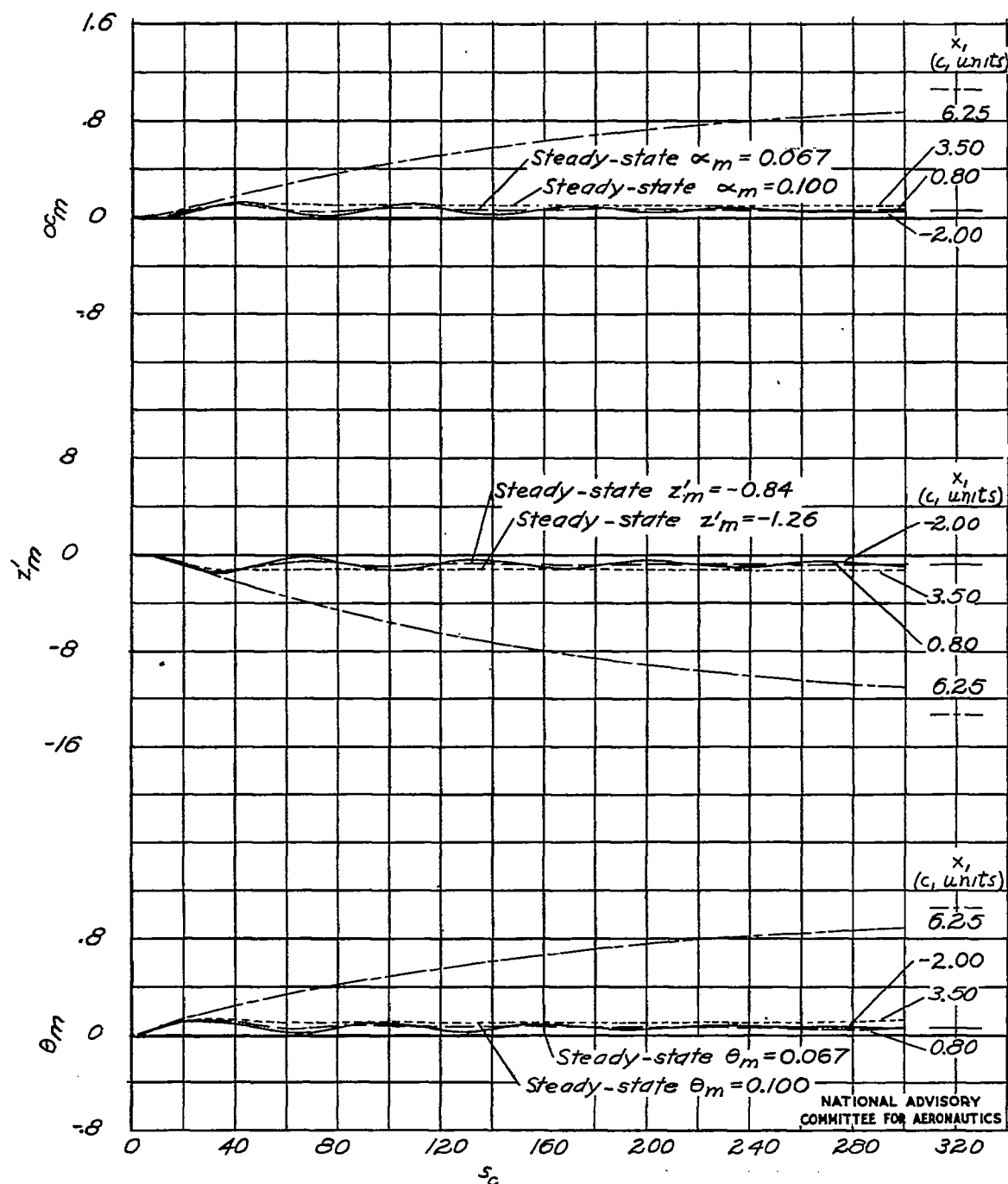
Figure 21.— Indicial responses for unit C_m disturbance. $\partial C_L/\partial z'$ double that for $\Gamma=30°$; $S_B=S_t$; $\epsilon=0$; $l=10.0c_i$; $K_y=6.67c_i$; $z_i=5.00c_i$; $x=-2.00c_i$, $0.80c_i$, $3.50c_i$, or $6.25c_i$.

Fig. 22   NACA TN No. 1285
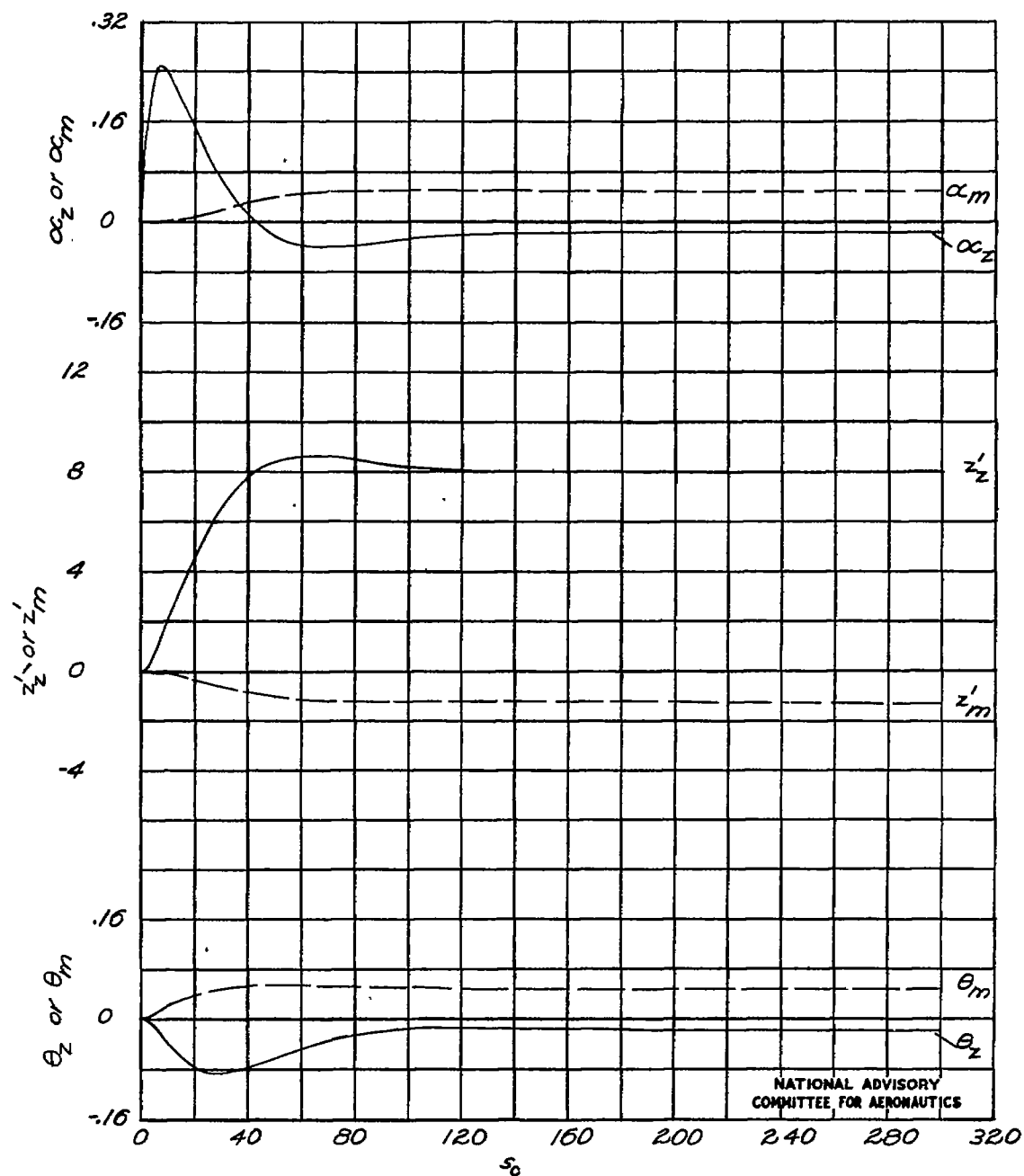
Figure 22.— Indicial responses for unit C_Z and unit C_m disturbances. $\Gamma = 30°$; $S_B = S_1$; $\epsilon = 0$; $l = 20.0\,c_1$; $z_o = 1.74\,c_1$; $K_y = 6.67\,c_1$; $z_1 = 5.00\,c_1$; $x_1 = 7.00\,c_1$.
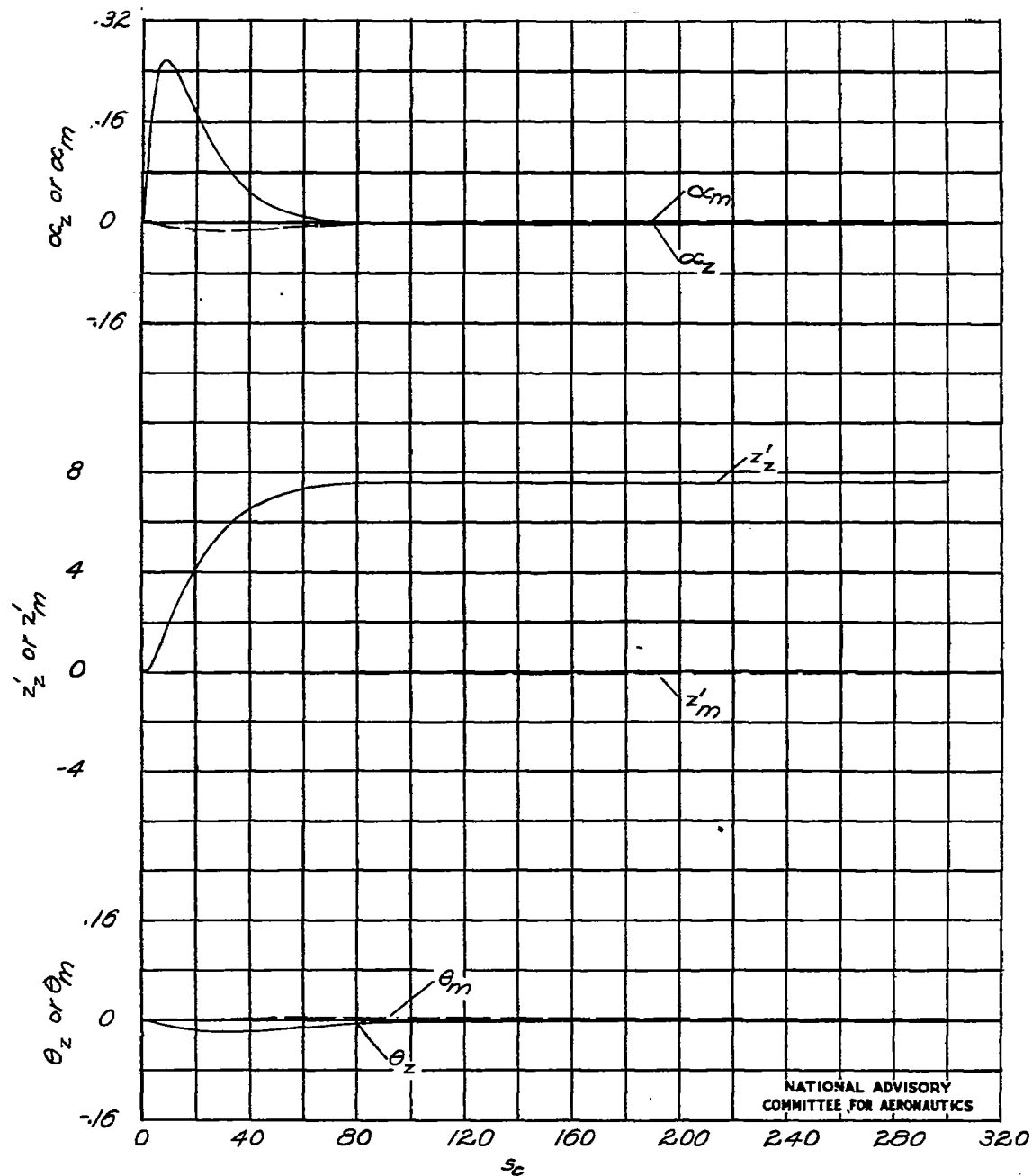
Figure 23.— Indicial responses for unit C_z and unit C_m disturbances. $\Gamma = 30°$; $S_2 = S_1$; $\epsilon = 0$; $l = 100.0\,c_1$; $z_0 = 1.74\,c_1$; $K_y = 6.67\,c_1$; $z_1 = 5.00\,c_1$; $x_1 = 35.00\,c_1$.

Fig. 24   NACA TN No. 1285

$$\rightarrow|10c_1|\leftarrow$$

$$|\leftarrow 20c_1 \rightarrow|$$

$$\leftarrow\!\!\!\!\!\!\!\!\!\!\!\!\!\!\!\!\!\! 100\,c_1 \!\!\!\!\!\!\!\!\!\!\!\!\!\!\!\!\!\!\rightarrow$$
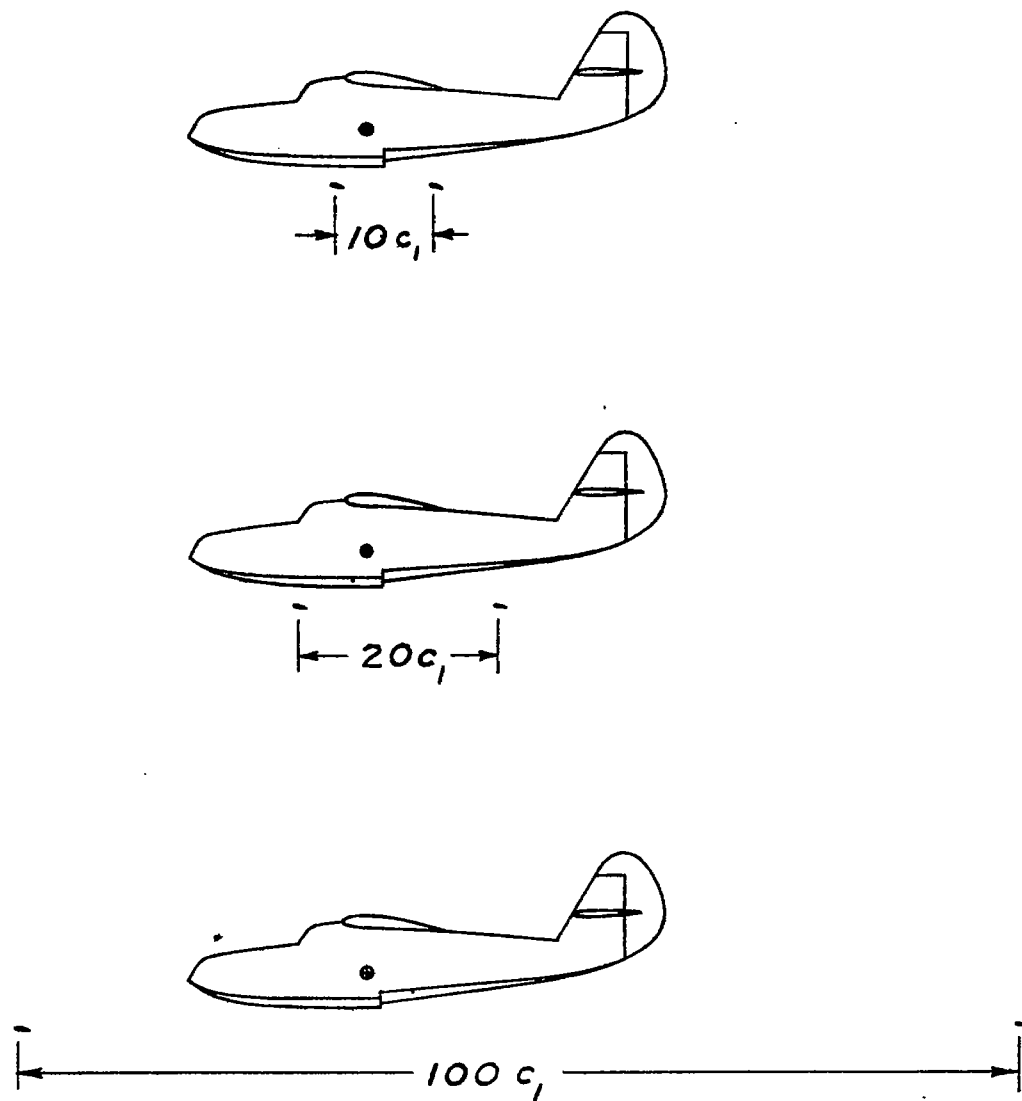
**NATIONAL ADVISORY
COMMITTEE FOR AERONAUTICS**

Figure 24.— Significance of longitudinal hydrofoil spacing on a typical flying boat.

Figure 25.-Positive senses of axes and motions.

Fig. 26   NACA TN No. 1285

Figure 26.- Variation of k with z_n for hydrofoil having rectangular plan form and rectangular tips. $A_n=6$; NACA 66,S-209 sections; $\Gamma_n=0°$; $c_n=5$ inches; V=20 feet per second.

Figure 27.- Variation of k_r with z_n for a hydrofoil having rectangular plan form and rectangular tips. $A_n = 6$; NACA 16-309 section; $\Gamma_n = 20°$ or $30°$; $c_n = 5$ inches; $V = 20$ feet per second.

Fig. 28   NACA TN No. 1285

Figure 28.- Variation of $1/(C_m)_{h=0}$ $\partial C_m/\partial h$ with h_o for a hydrofoil having rectangular plan form and rectangular tips; $h_t=0$; NACA 66,5-209 section; $h_t=0$; $C_h=3$ inches; $V=20$ feet per second.

Figure 29.- Variation of $\partial (C_L)_n / \partial \alpha_n$ with z_{o_n} for a hydrofoil having rectangular plan form and rectangular tips. $A_n=6$; NACA 16-509 section; $\Gamma_n=0°, 20°,$ or $30°$; $c_n=5$ inches; $V=20$ feet per second.

Fig. 30   NACA TN No. 1285

Figure 30.- Variation of k_2 and k_3 with z_n for a hydrofoil having rectangular plan form and rectangular tips. $A_n = 6$; NACA 66,5-209 section; $i_n = 0°$; $c_n = 5$ inches; $V = 20$ feet per second.

Figure 31.- Variation of k_2 and k_3 with z_n for a hydrofoil having rectangular plan form and rectangular tips. $A=6$; NACA 16-509 section; $\Gamma_n = 30°$; $c_n = 5$ inches; $V = 20$ feet per second.

Fig. 32   NACA TN No. 1285

Figure 32.- Variation of k_s and k_s with z_{o_n} for a hydrofoil having rectangular plan form and rectangular tips. $\Lambda_n=0$; NACA 66,S-209 section; $\Gamma_n=0°$; $c_n=5$ inches; $V=20$ feet per second.

NATIONAL ADVISORY
COMMITTEE FOR AERONAUTICS

Figure 33.- Variation of k_4 and k_5 with z_{o_n} for a hydrofoil having rectangular plan form and rectangular tips. $\Lambda_n = 0$; NACA 16-509 section; $\Gamma_n = 30°$; $c_n = 3$ inches; $V = 20$ feet per second.

Fig. 34

Figure 34.- Variation of (C_{D_i}) with (C_L) for a horizontal moving rectangular, elliptic, flared and rectangular tips. $A_1 = 6$; NACA 66,S-209 section; $i_n = 0°$; $c_n = 5$ inches; $V = 20$ feet per second.

Figure 35.- Variation of $(C_D)_n$ with $(C_L)_n$ for a hydrofoil having rectangular plan form and rectangular tips. $A_n = 6$; NACA 16-509 section; $\Gamma_n = 0°$; $c_n = 3$ inches; $V = 20$ feet per second.

Fig. 35

Fig. 36

Figure 36.- Variation of $\partial(c_l)_n / \partial \alpha_n$ and y_{c_n} with f_n.

Figure 37.- Variation of r_h with F_R.